NATIONAL CANCER INSTITUTE

PHYSICAL SCIENCES — in ONCOLOGY

THE SCRIPPS RESEARCH INSTITUTE

USC VITERBI SCHOOL OF ENGINEERING

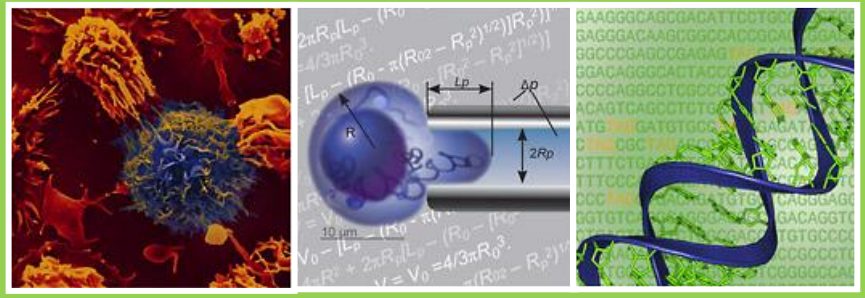

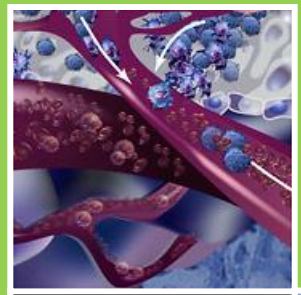

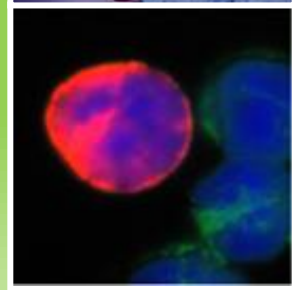

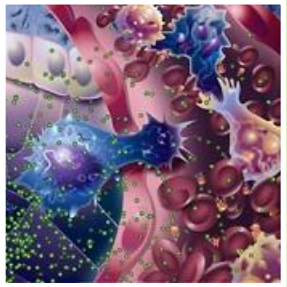

Cancer metastasis modeling at the Scripps Physical Science Oncology Center

-Overview of several projects-

Paul K. Newton Ph.D.

Viterbi School of Engineering and Department of Mathematics
University of Southern California

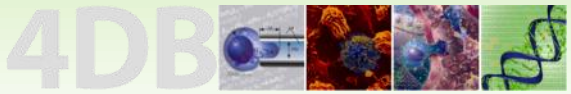

Overview of models

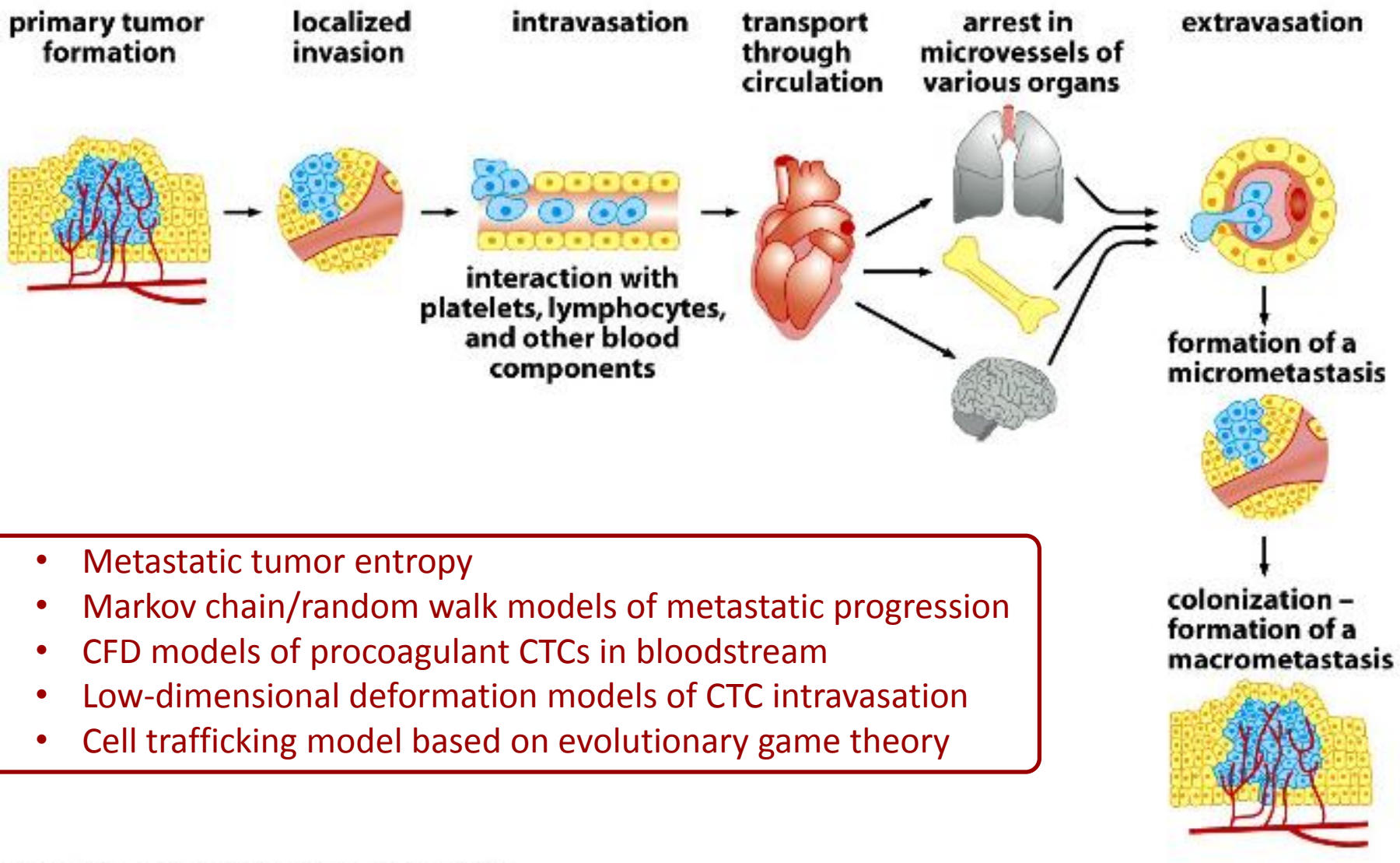

- Metastatic tumor entropy
- Markov chain/random walk models of metastatic progression
- CFD models of procoagulant CTCs in bloodstream
- Low-dimensional deformation models of CTC intravasation
- Cell trafficking model based on evolutionary game theory

Figure 14-4 The Biology of Cancer (© Garland Science 2007)

PHYSICAL SCIENCES-ONCOLOGY CENTERS





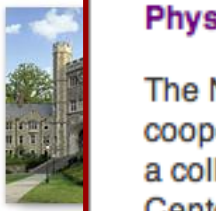
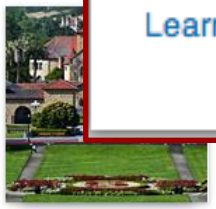

Arizona State University

Cornell University

CENTERS

-John Niederhuber M.D. 2006-2010
- Harold Varmus M.D. 2010-

Physical Science-Oncology Centers

The National Cancer Institute (NCI) has awarded cooperative agreements to 12 leading institutions to build a collaborative network of Physical Science-Oncology Centers (PS-OCs).

Learn More »

ology Center
a, NY
chael L. Shuler, Ph.D.
rbara L. Hempstead,

enter & Research
ology Center
enter & Research
bert A. Gatenby, M.D.
bert J. Gillies, Ph.D.

of Technology
ology Center
of Technology,
ott Manalis, Ph.D.
er Jacks, Ph.D.

ology Center
, Chicago, IL
omas V. O'Halloran,
nathan D. Licht, M.D.

nstitute
ology Center
nstitute, La Jolla, CA
ter Kuhn, Ph.D.
lly J. Bethel, M.D.

California
ology Center
California, Los
Daniel Hillis, Ph.D.
vid B. Agus, M.D.

View Now »

Scripps PS-OC: `Mathematics and Physics of Cancer Metastasis'

Physical Sciences Oncology Center 2010-2015 National Cancer Institute

Mathematics & Physics


Peter Kuhn


Paul Newton


Owen McCarty

Oncology and Pathology


Kelly Bethel


Jorge Nieva


Lyudmila Bazhenova

Collaborators

Math Modeling - USC

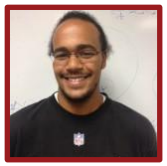
Jeremy Mason


Angie Lee


Jeffrey West

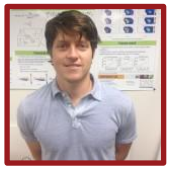
Brian Hurt


Zaki Hasnain


Juliana Porter

MSKCC


Larry Norton

The `particles' in the bloodstream

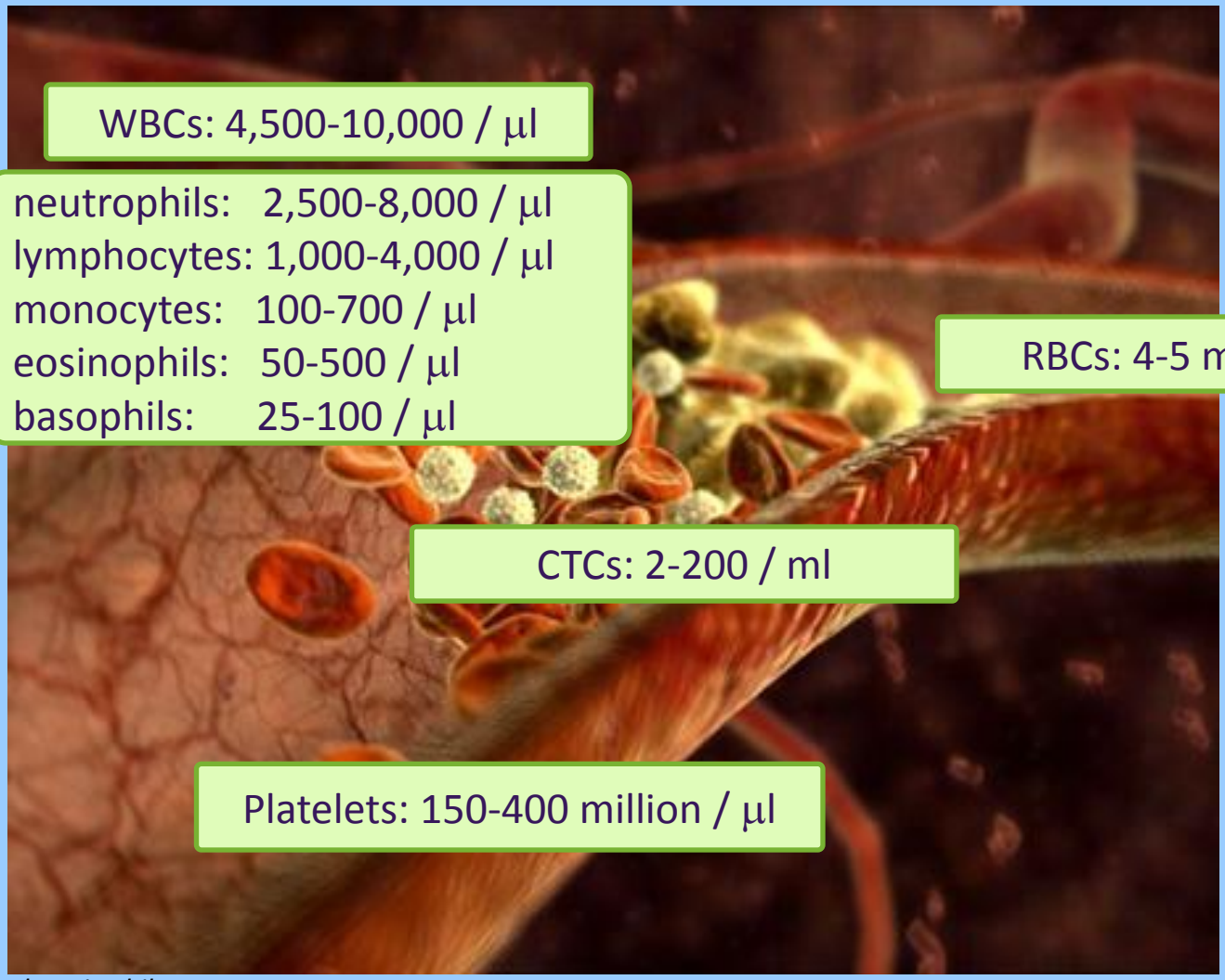

Phoenix Philms

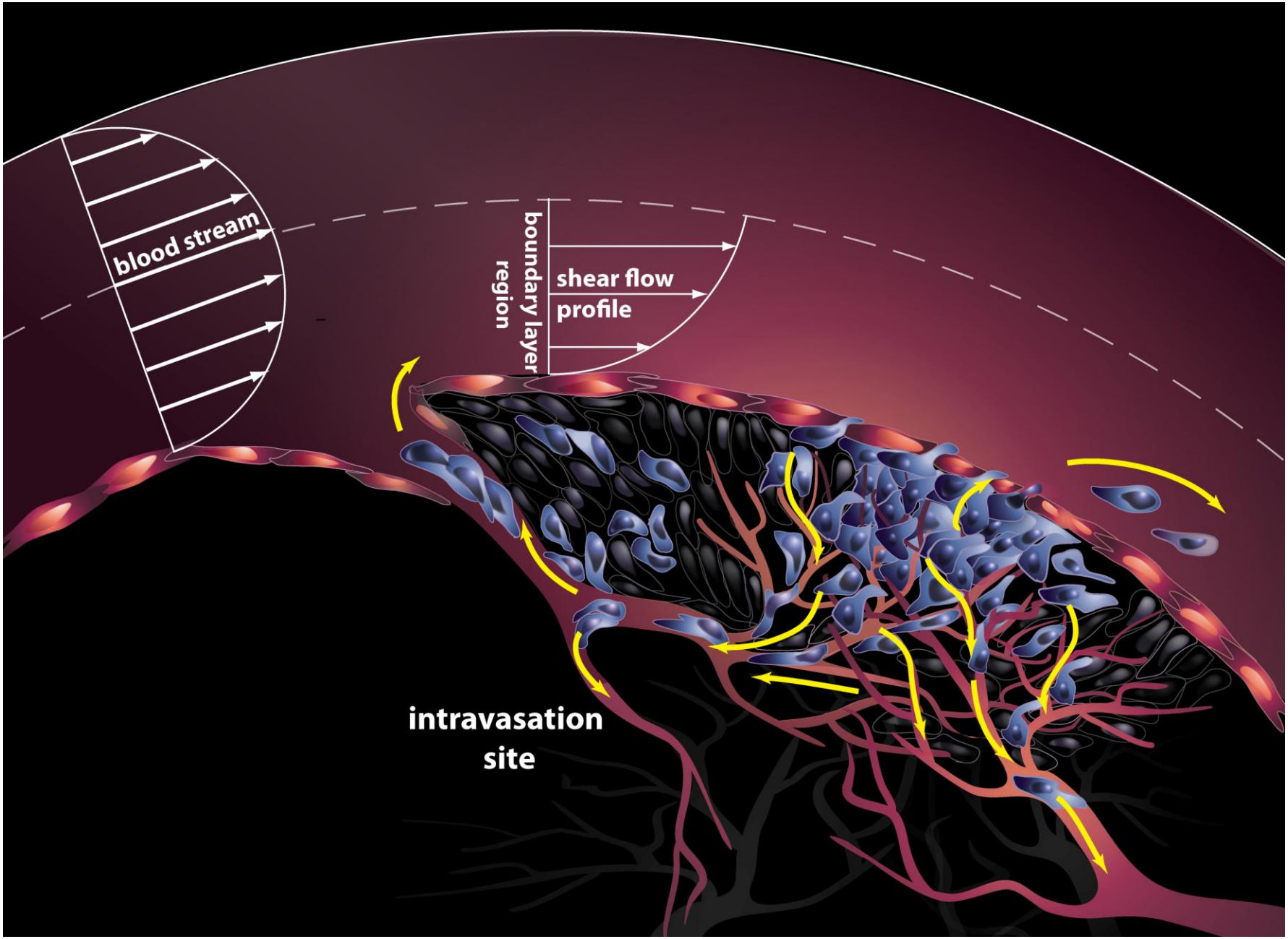
blood stream
boundary layer region
shear flow profile
intravasation site

T.R. Ashworth 1869

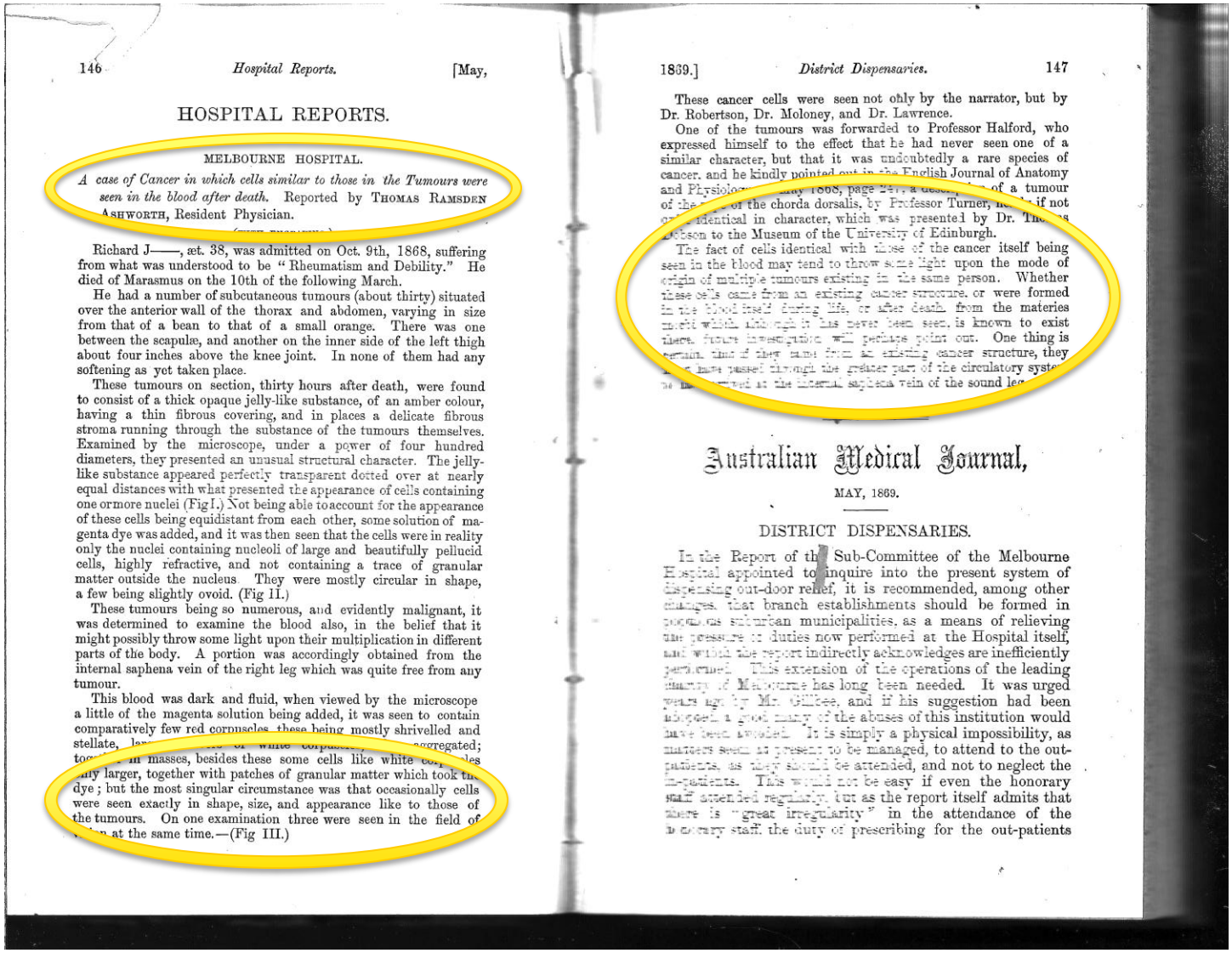

146 *Hospital Reports.* [May,

HOSPITAL REPORTS.

MELBOURNE HOSPITAL.

A case of Cancer in which cells similar to those in the Tumours were seen in the blood after death. Reported by THOMAS RAMSDEN ASHWORTH, Resident Physician.

Richard J——, æt. 38, was admitted on Oct. 9th, 1868, suffering from what was understood to be "Rheumatism and Debility." He died of Marasmus on the 10th of the following March.

He had a number of subcutaneous tumours (about thirty) situated over the anterior wall of the thorax and abdomen, varying in size from that of a bean to that of a small orange. There was one between the scapulæ, and another on the inner side of the left thigh about four inches above the knee joint. In none of them had any softening as yet taken place.

These tumours on section, thirty hours after death, were found to consist of a thick opaque jelly-like substance, of an amber colour, having a thin fibrous covering, and in places a delicate fibrous stroma running through the substance of the tumours themselves. Examined by the microscope, under a power of four hundred diameters, they presented an unusual structural character. The jelly-like substance appeared perfectly transparent dotted over at nearly equal distances with what presented the appearance of cells containing one or more nuclei (Fig I.) Not being able to account for the appearance of these cells being equidistant from each other, some solution of magenta dye was added, and it was then seen that the cells were in reality only the nuclei containing nucleoli of large and beautifully pellucid cells, highly refractive, and not containing a trace of granular matter outside the nucleus. They were mostly circular in shape, a few being slightly ovoid. (Fig II.)

These tumours being so numerous, and evidently malignant, it was determined to examine the blood also, in the belief that it might possibly throw some light upon their multiplication in different parts of the body. A portion was accordingly obtained from the internal saphena vein of the right leg which was quite free from any tumour.

This blood was dark and fluid, when viewed by the microscope a little of the magenta solution being added, it was seen to contain comparatively few red corpuscles, these being mostly shrivelled and stellate, la[illegible] of white corpuscles, [illegible]aggregated; to[illegible] in masses, besides these some cells like white co[illegible]les ...ny larger, together with patches of granular matter which took th... dye; but the most singular circumstance was that occasionally cells were seen exactly in shape, size, and appearance like to those of the tumours. On one examination three were seen in the field of [illegible]n at the same time.—(Fig III.)

1869.] *District Dispensaries.* 147

These cancer cells were seen not only by the narrator, but by Dr. Robertson, Dr. Moloney, and Dr. Lawrence.

One of the tumours was forwarded to Professor Halford, who expressed himself to the effect that he had never seen one of a similar character, but that it was undoubtedly a rare species of cancer, and he kindly pointed out in the English Journal of Anatomy and Physiol[illegible] May 1868, page 241, a desc[illegible] of a tumour of the [illegible] of the chorda dorsalis, by Professor Turner, [illegible] if not ...identical in character, which was presented by Dr. Tho[illegible]s ...bson to the Museum of the University of Edinburgh.

The fact of cells identical with those of the cancer itself being seen in the blood may tend to throw some light upon the mode of origin of multiple tumours existing in the same person. Whether these cells came from an existing cancer structure, or were formed in the blood itself during life, or after death, from the materies morbi within although it has never been seen, is known to exist there, future investigations will perhaps point out. One thing is certain, that if they came from an existing cancer structure, they [illegible] have passed through the greater part of the circulatory syste[illegible] ...ed at the internal saphena vein of the sound leg.

Australian Medical Journal,

MAY, 1869.

DISTRICT DISPENSARIES.

In the Report of the Sub-Committee of the Melbourne Hospital appointed to inquire into the present system of dispensing out-door relief, it is recommended, among other changes, that branch establishments should be formed in populous suburban municipalities, as a means of relieving the pressure of duties now performed at the Hospital itself, and which the report indirectly acknowledges are inefficiently performed. This extension of the operations of the leading charity of Melbourne has long been needed. It was urged years ago by Mr. Gillbee, and if his suggestion had been adopted a great many of the abuses of this institution would have been avoided. It is simply a physical impossibility, as matters seem at present to be managed, to attend to the out-patients, as they should be attended, and not to neglect the in-patients. This would not be easy if even the honorary staff attended regularly, but as the report itself admits that there is "great irregularity" in the attendance of the honorary staff, the duty of prescribing for the out-patients

HD-CTC on a slide (Kuhn Lab TSRI)

~3 Million Cells per slide

3-30 CTCs per slide

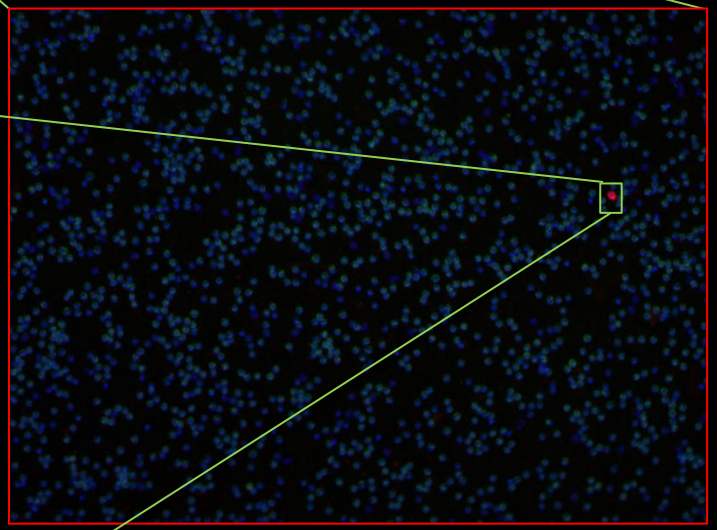

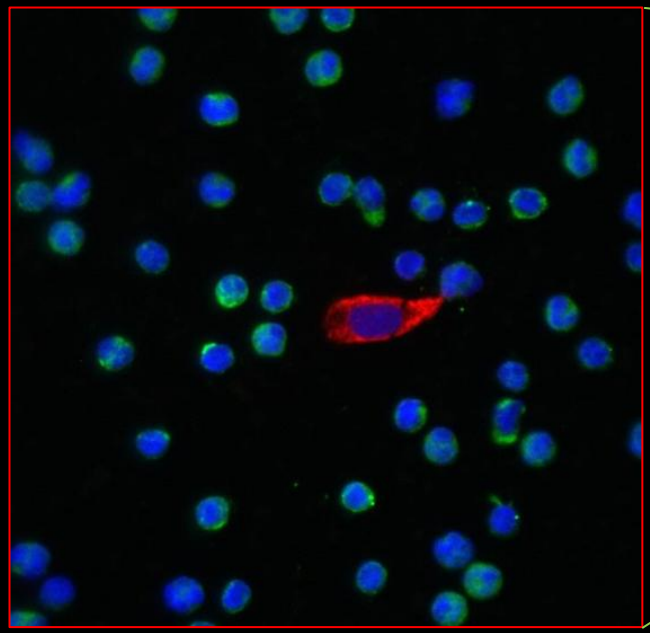

Circulating tumor cells (CTCs)

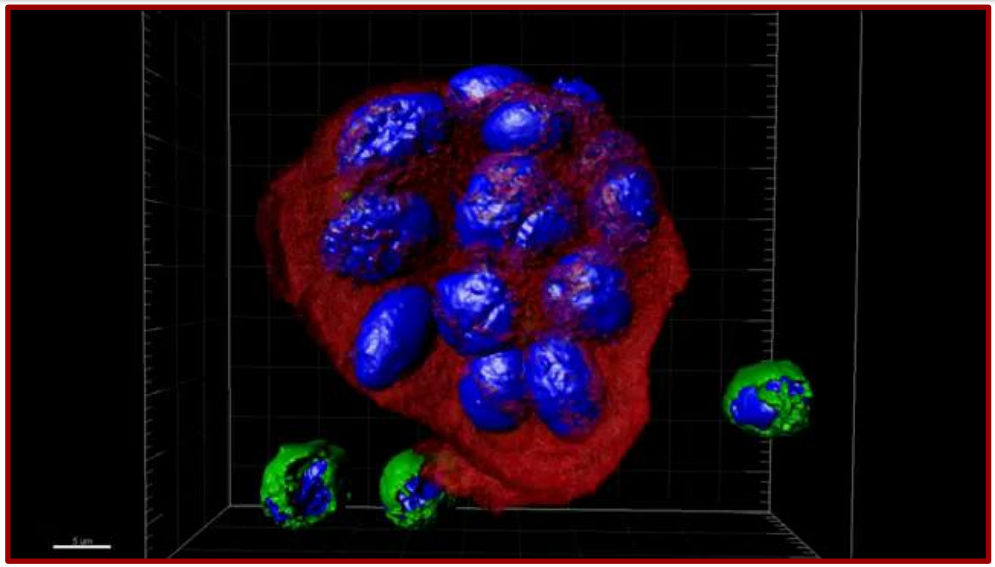

Lung CTC cluster

Prostate CTCs

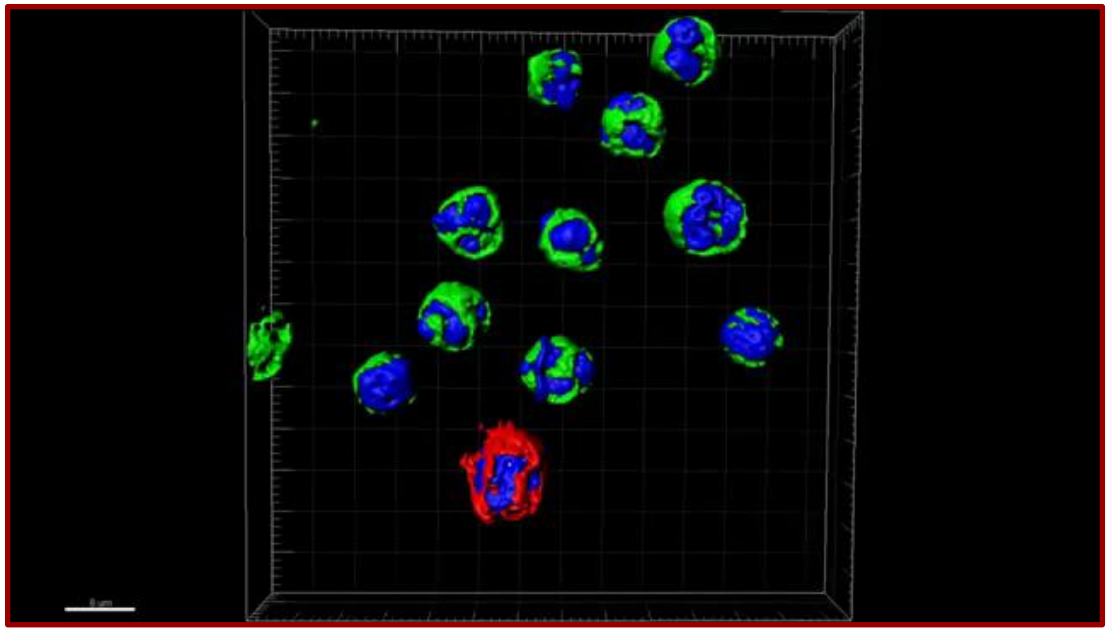

Peter Kuhn Lab
The Scripps Research Institute

1. Metastatic entropy

Question: What is the best metric to use to compare the complexity of different cancers?

Metastatic signature of 4 cancer types

Lung

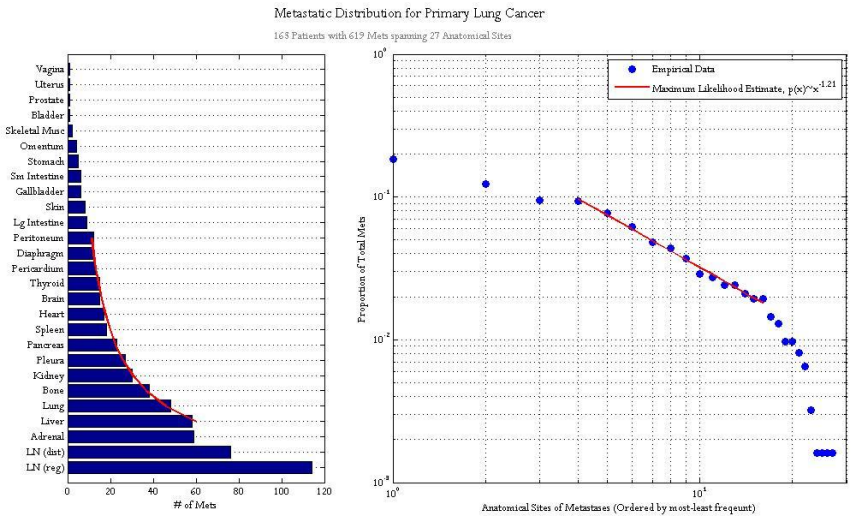

Breast

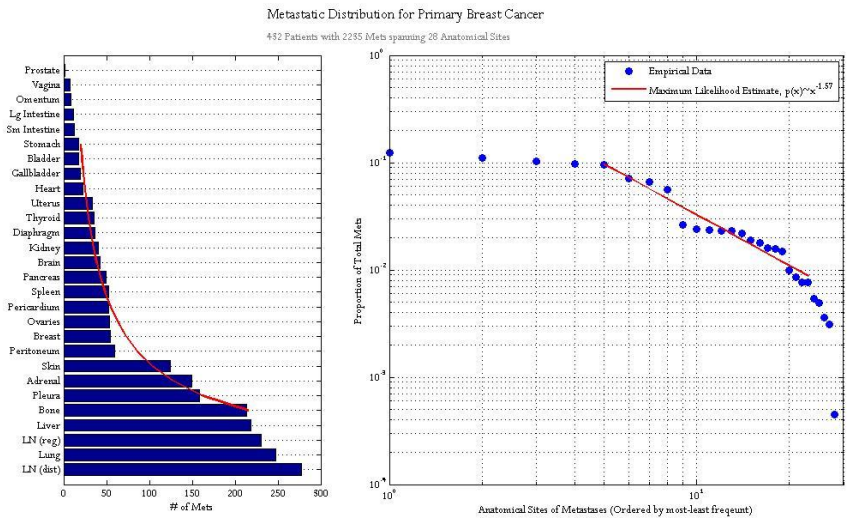

Prostate

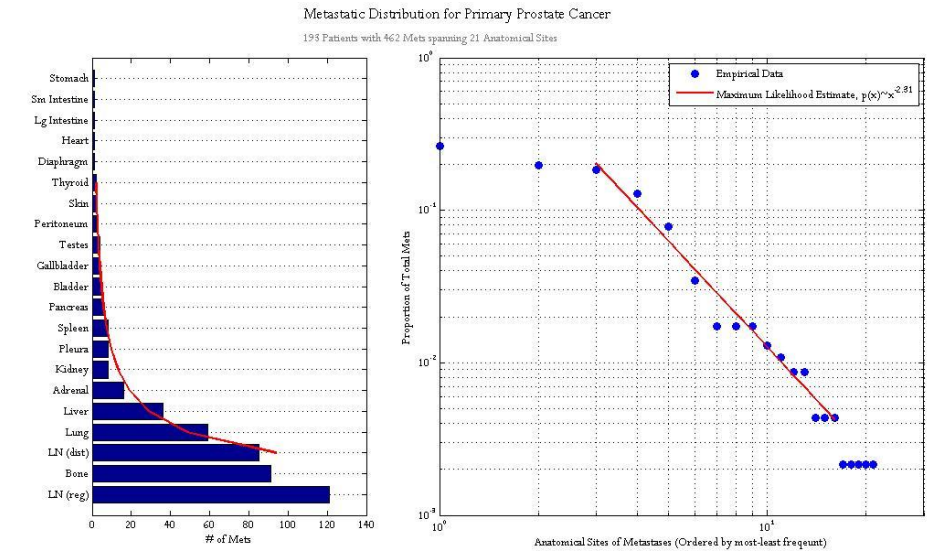

Colon

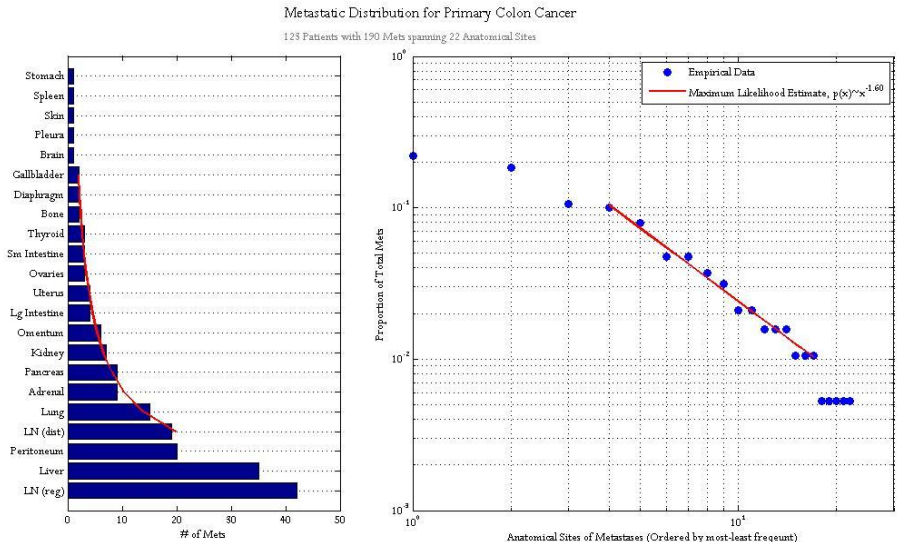

Metastatic entropy

Two main `drivers' of metastatic complexity

1. Number of metastatic sites `N'
   - Larger N increases complexity

2. Probabilistic distribution to those sites
   - More even distribution (flatter) increases complexity

Metastatic entropy

$$E_N = -\sum_{i=1}^{N} p_i \log p_i$$

p_i % metastatic tumors to site `i'

Metastatic entropy

$$0 \leq E_N \leq \log N$$

Initial state: Primary tumor, no mets

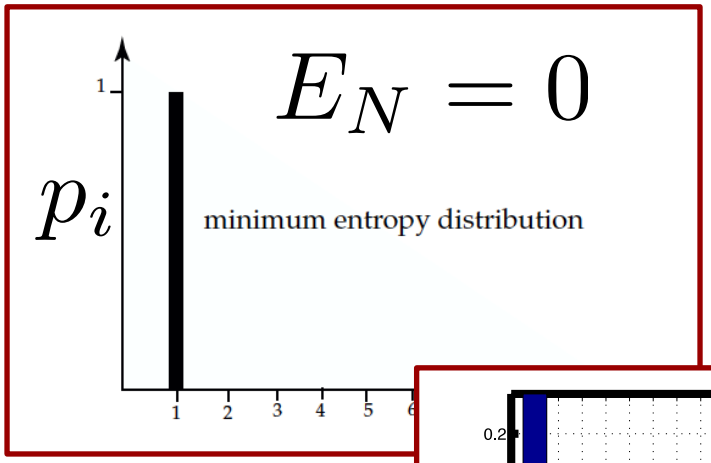

Hypothetical state: Worst case scenario

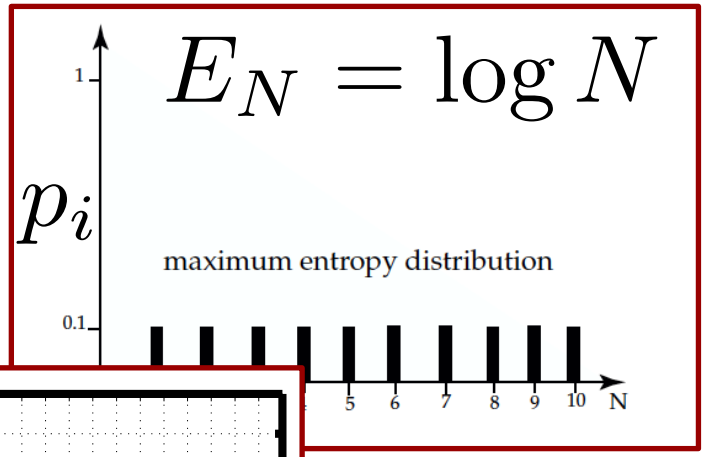

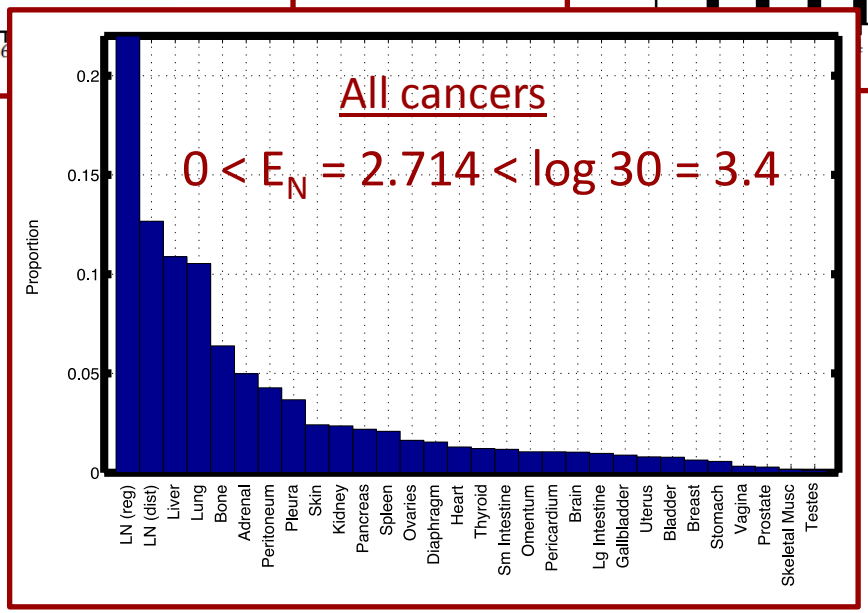

Tumor entropy

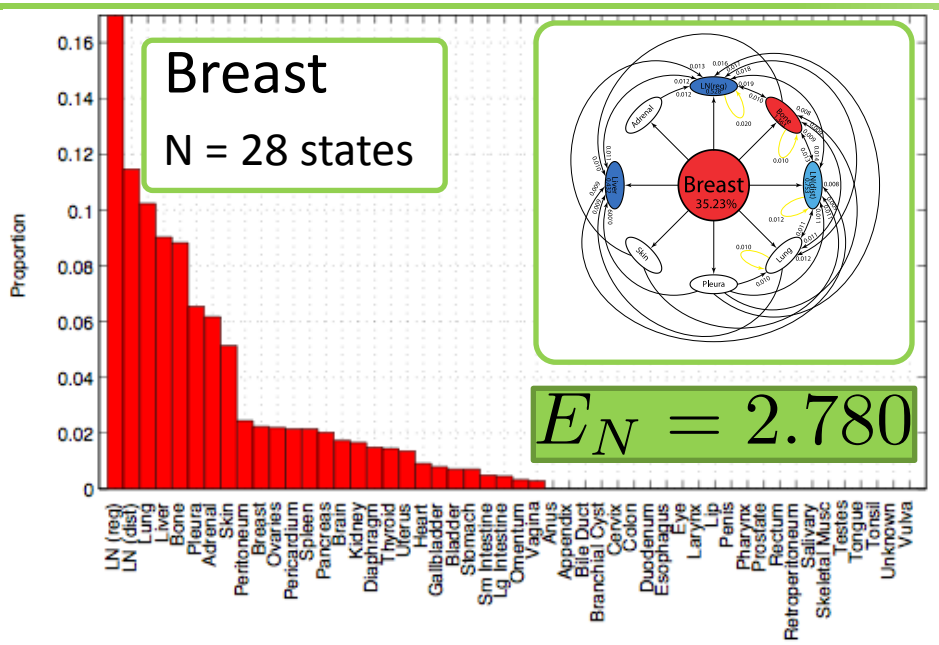

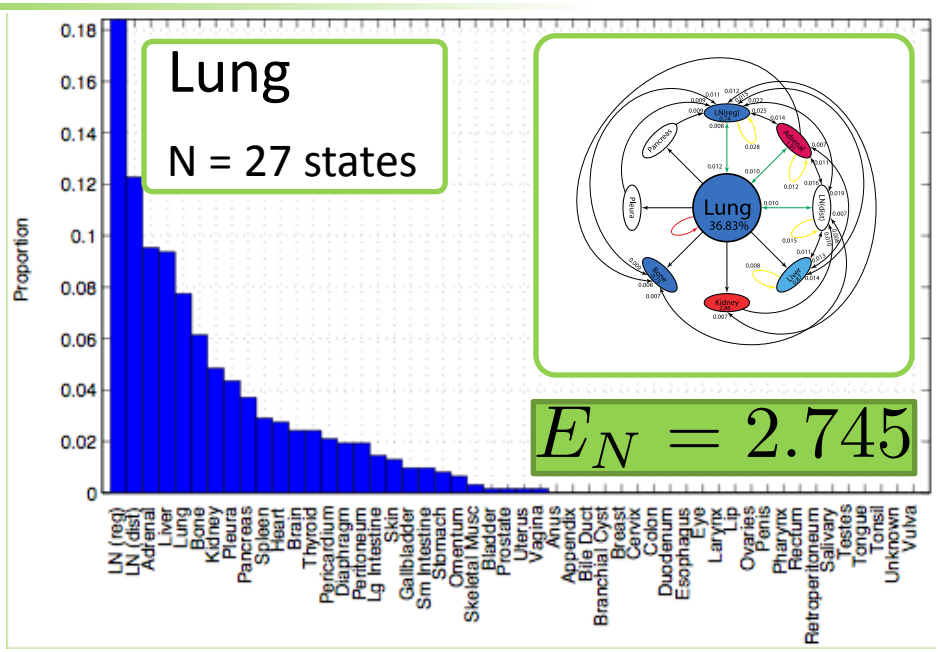

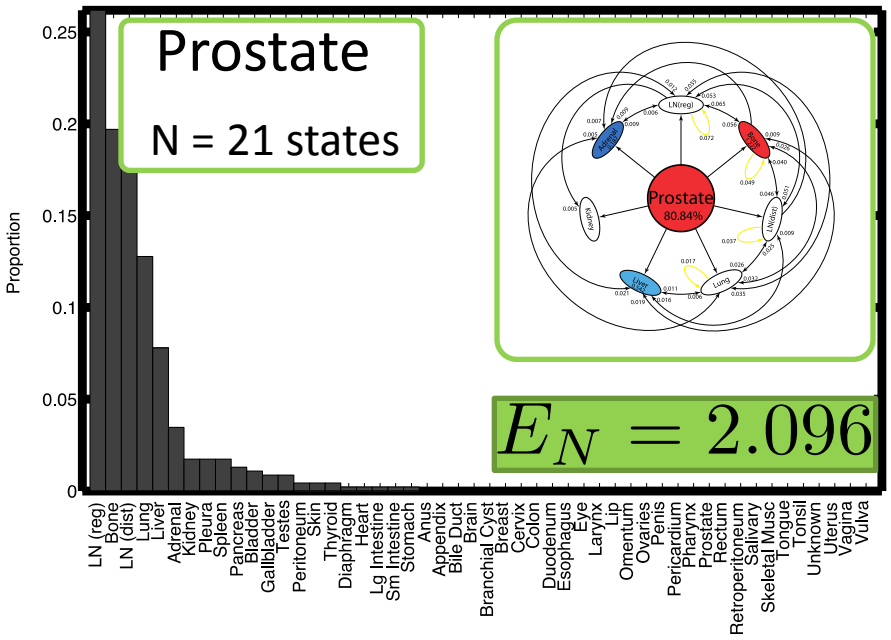

Tumor entropy

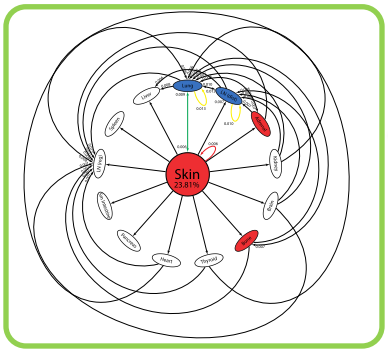

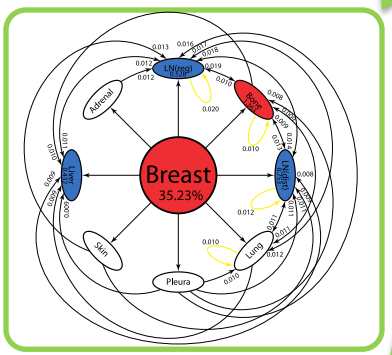

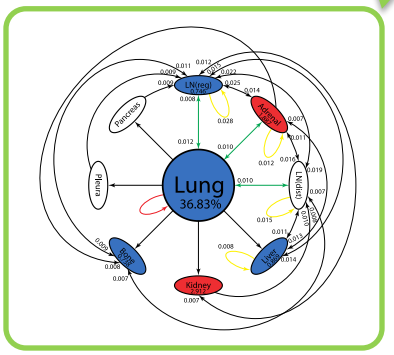

Primary	N	Entropy
Skin	30	2.9945
Breast	27	2.7798
Kidney	27	2.7554
Lung	27	2.7453
All	30	2.7136
Stomach	28	2.6099
Uterine	24	2.5709
Pancreatic	26	2.5540
Colorectal	28	2.4686
Cervical	26	2.3696
Ovarian	21	2.3275
Bladder	22	2.2301
Prostate	21	2.0960

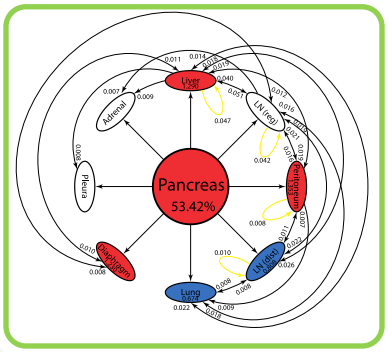

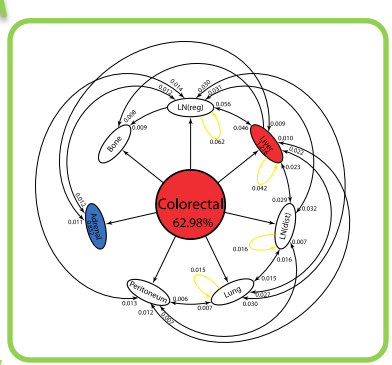

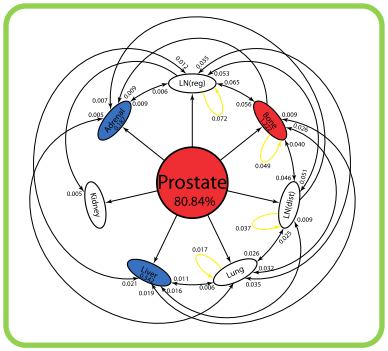

2. Markov chain/random walk models of metastatic progression

Question: What is the dynamical system that *drives* metastatic progression from a state of low-entropy to a high-entropy state?

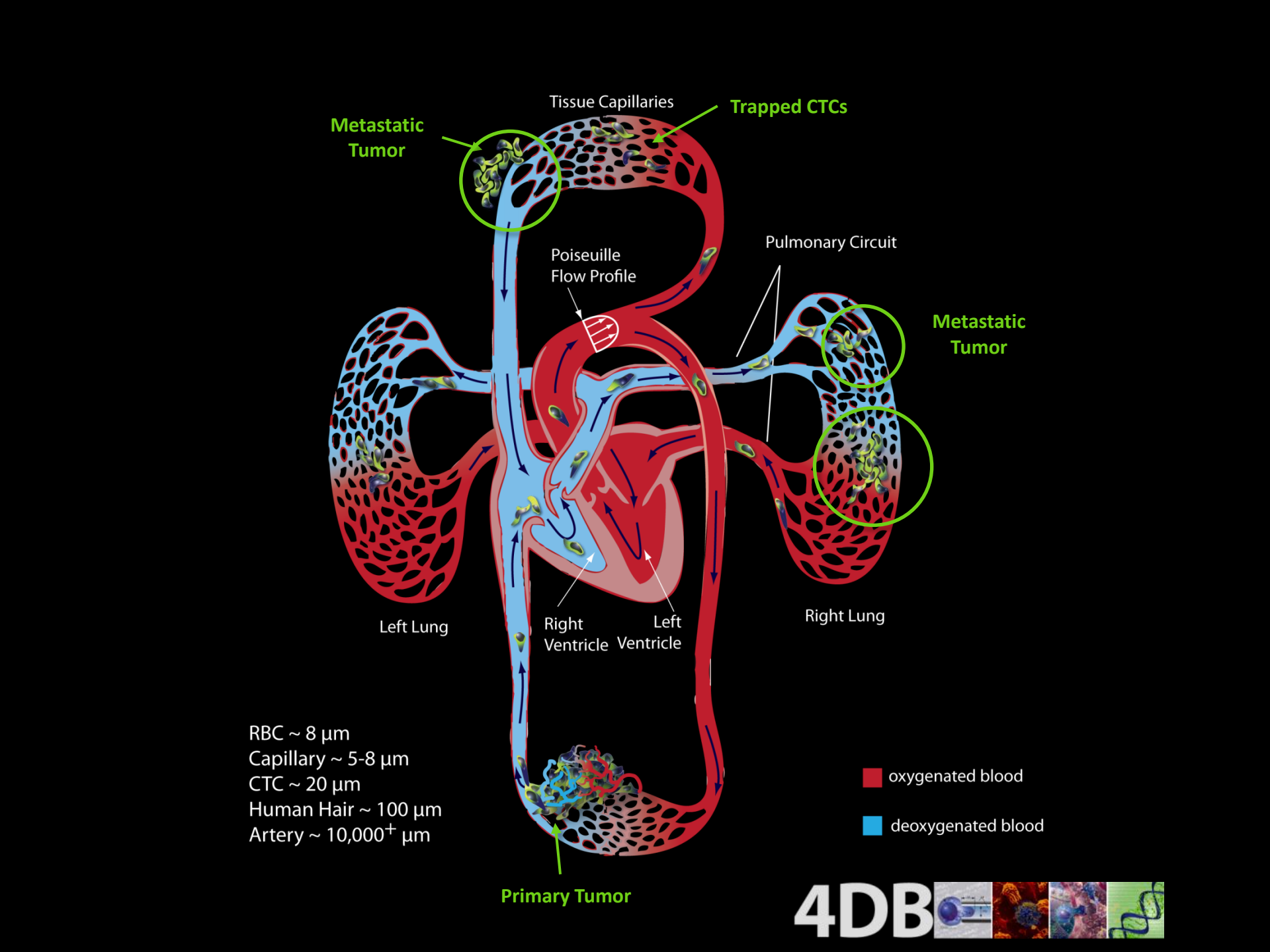
Tissue Capillaries
Trapped CTCs
Metastatic Tumor
Poiseuille Flow Profile
Pulmonary Circuit
Metastatic Tumor
Left Lung
Right Ventricle
Left Ventricle
Right Lung
RBC ~ 8 µm
Capillary ~ 5-8 µm
CTC ~ 20 µm
Human Hair ~ 100 µm
Artery ~ 10,000+ µm
oxygenated blood
deoxygenated blood
Primary Tumor
4DB

Google's Markov model

Random walkers on an IT network

Google Search

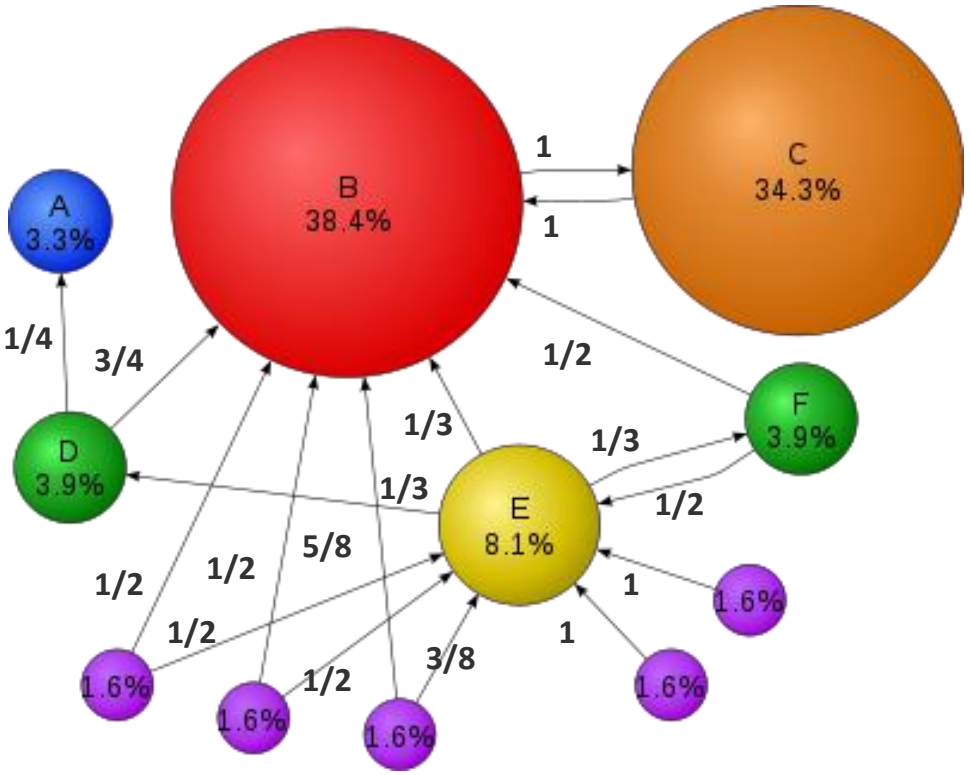

Edge Weights: `Transition' probabilities

Main features:

- Nodes are web pages
- Nodes are linked by directed edges
- Edges have weights (transition probabilites)
- Nodal weights are obtained from edge weights

Google uses the internet model to:

- Perform simulated internet searches:
  - Individual searches with random walks
  - `Ensemble' searches with Monte Carlo simulations
- Run tests under different scenarios
- Calculate `average' number of steps from node i to node j

Our Cancer Progression Model

Random walkers on an anatomical network

Lung cancer

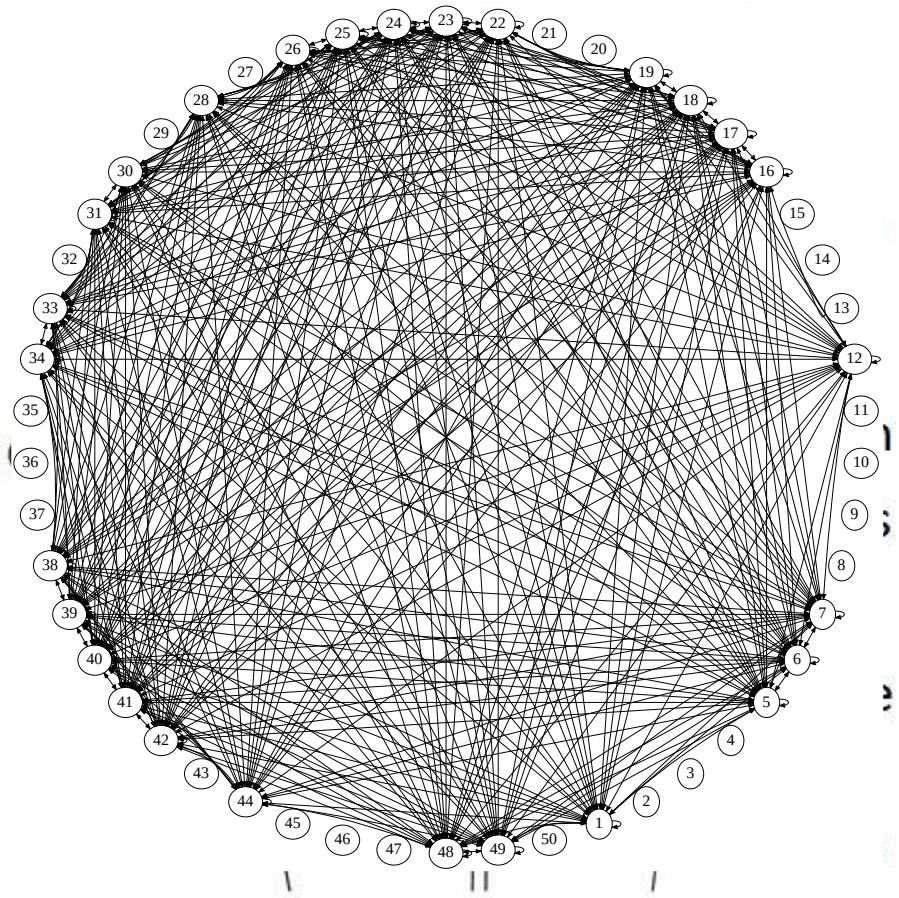

Main features:

- Nodes are potential tumor sites
- Nodes are linked by directed edges
- Need to construct the edge weights

Similar uses for our model:

- Perform simulated cancer progression:
  - Individual progression with random walks
  - `Ensemble' progression with Monte Carlo simulations
- Run tests under different scenarios
- Calculate `average' number of steps from node i to node j (mean first-passage times)

Markov Chain Basics

$$\vec{v}_{k+1} = \vec{v}_k A, (k = 0, 1, 2, ...)$$

- States: Lung, Breast, Liver, Adrenal, LN, ….Deceased
- Initial state: $\vec{v}_0 =$ (1,0,0,0,….)
- Steady-state: $\vec{v}_\infty =$ (0.18, 0.12, ….)

$\vec{v}_k$ is the state-vector with 50 entries reflecting possible metastatic tumor locations

- A is the transition matrix governing the transition probabilities from site to site

How to compute (estimate) the entries of the transition matrix A?

- Need *the transition probabilities* from site to site:
  - Reconstruct from steady-state info (autopsy data sets)
  - Direct empirical calculation (longitudinal data sets)

The Lung Cancer Network

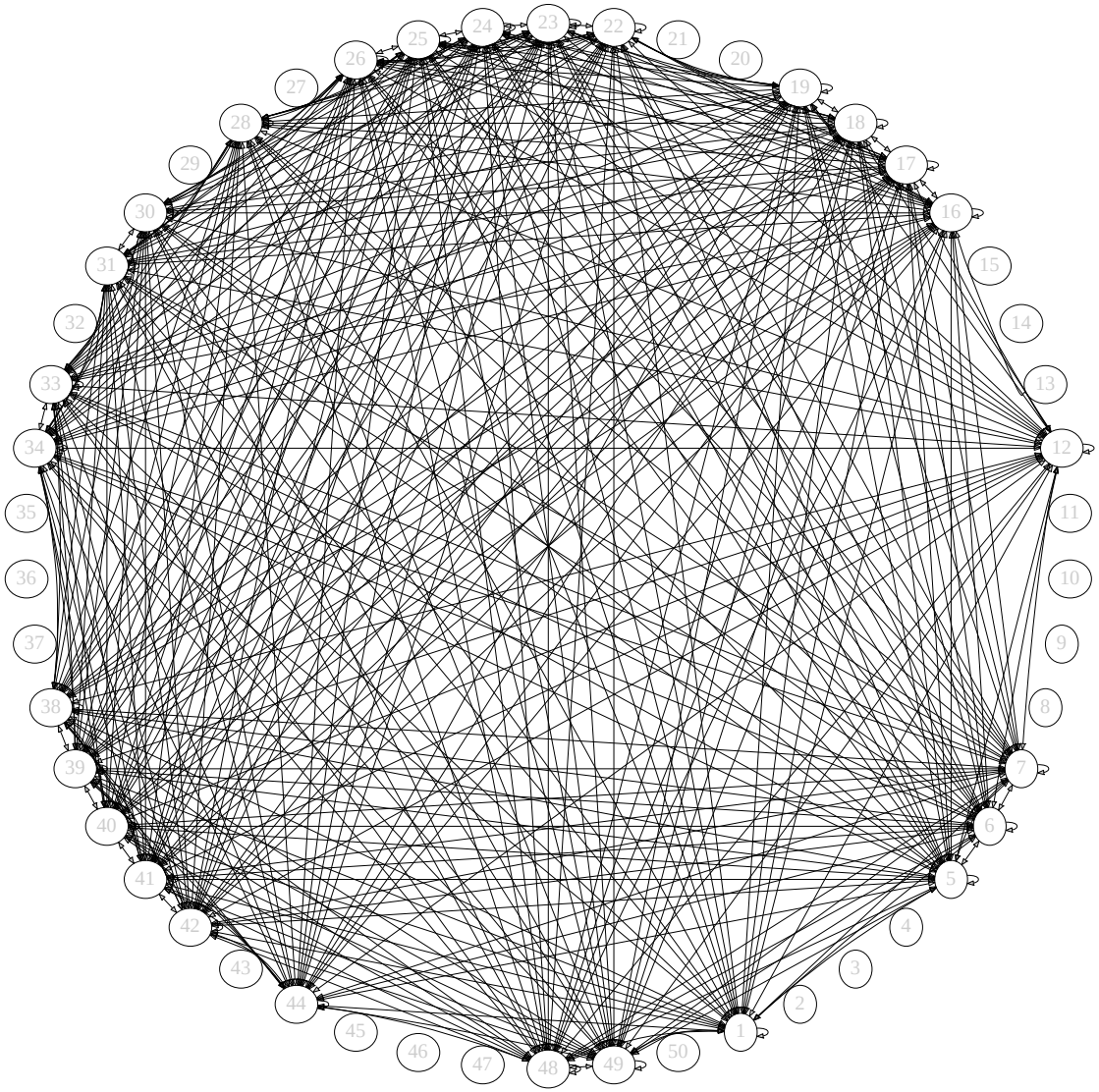

- 913 edges
- Lung: 27 outgoing edges
- Lung: 49 incoming edges

#	Name	#	Name
1	Adrenal	26	Omentum
2	Anus	27	Ovaris
3	Appendix	28	Pancreas
4	Bile Duct	29	Penis
5	Bladder	30	Pericardium
6	Bone	31	Peritoneum
7	Brain	32	Pharynx
8	Branchial Cyst	33	Pleura
9	Breast	34	Prostate
10	Cervix	35	Rectum
11	Colon	36	Retroperitoneum
12	Diaphragm	37	Salivary
13	Duodenum	38	Skeletal Muscle
14	Esophagus	39	Skin
15	Eye	40	Small Intestine
16	Gallbladder	41	Spleen
17	Heart	42	Stomach
18	Kidney	43	Testes
19	Large Intestine	44	Thyroid
20	Larynx	45	Tongue
21	Lip	46	Tonsil
22	Liver	47	Unknown
23	Lung	48	Uteris
24	Lymph Nodes (reg)	49	Vagina
25	Lymph Nodes (dist)	50	Vulva

Convergence: Lung cancer

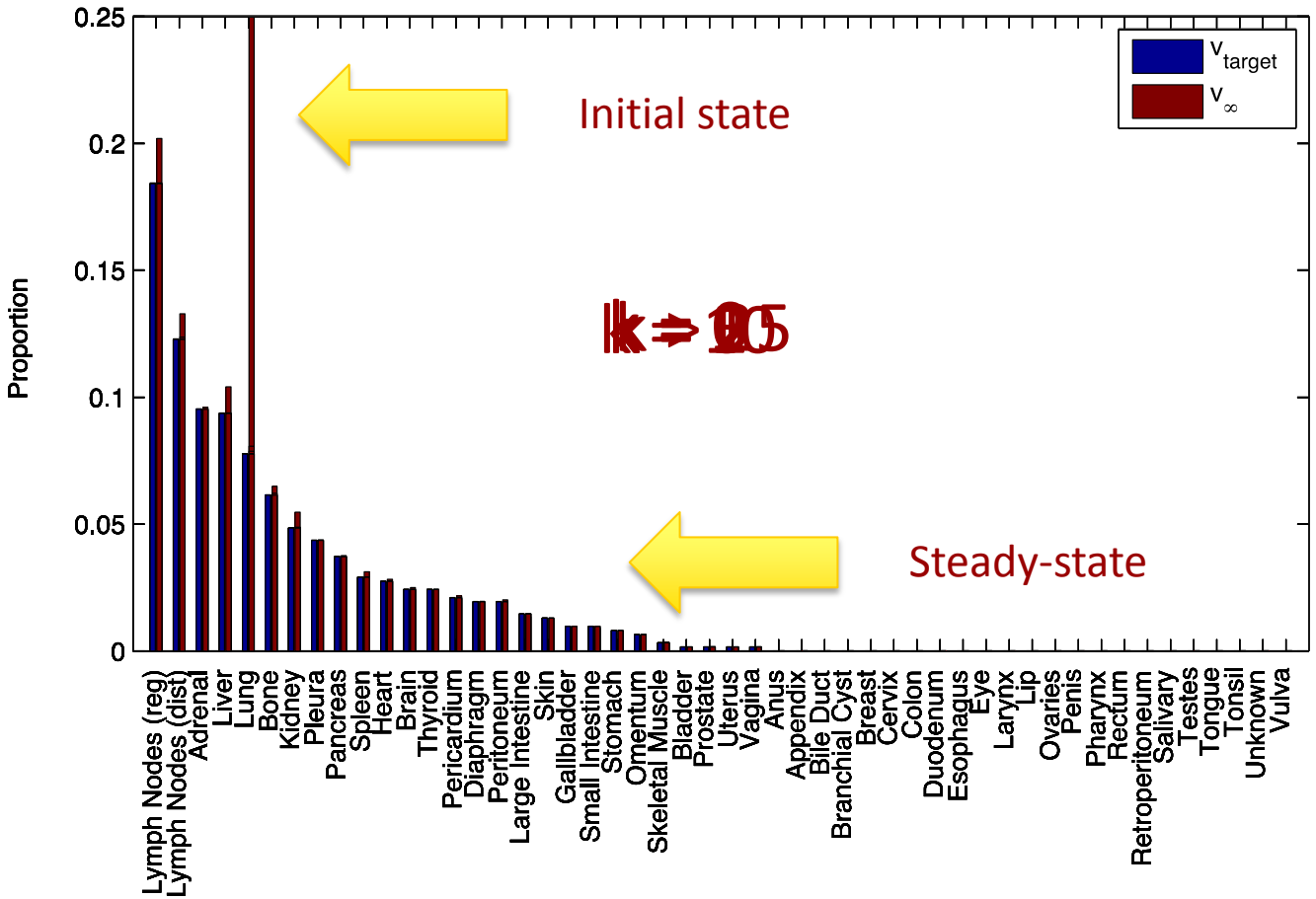

Network diagrams for 4 cancer types

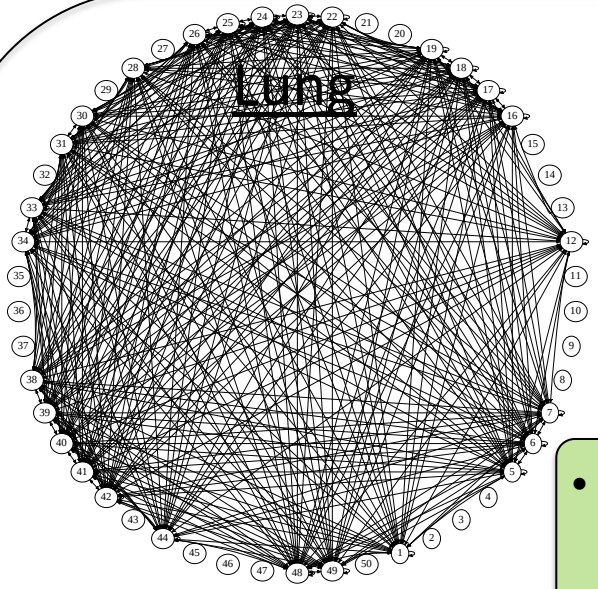

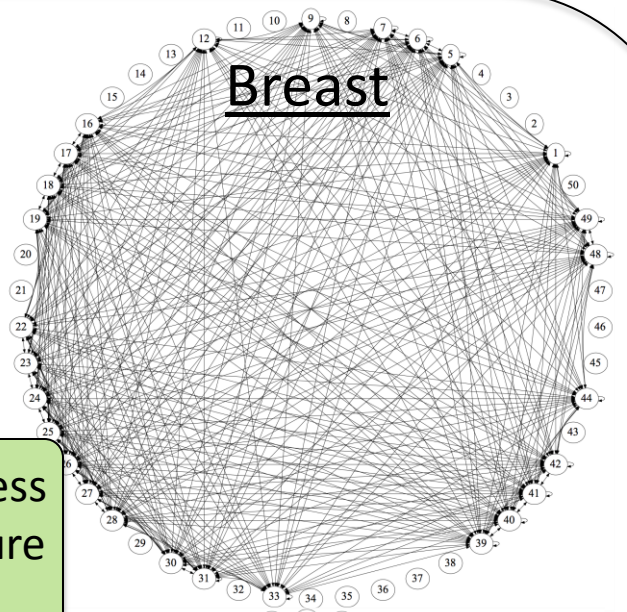

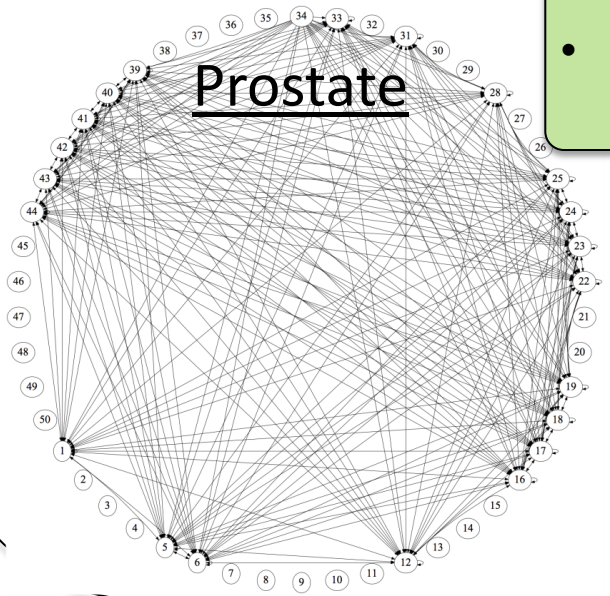

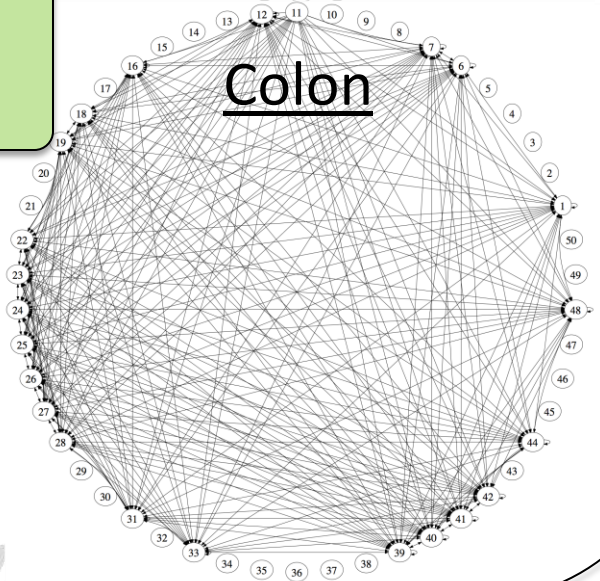

- Network inter-connectedness highlights the *systemic* nature of the disease
- Network *density* reflects relative complexity

Nearly complete convergence in two steps

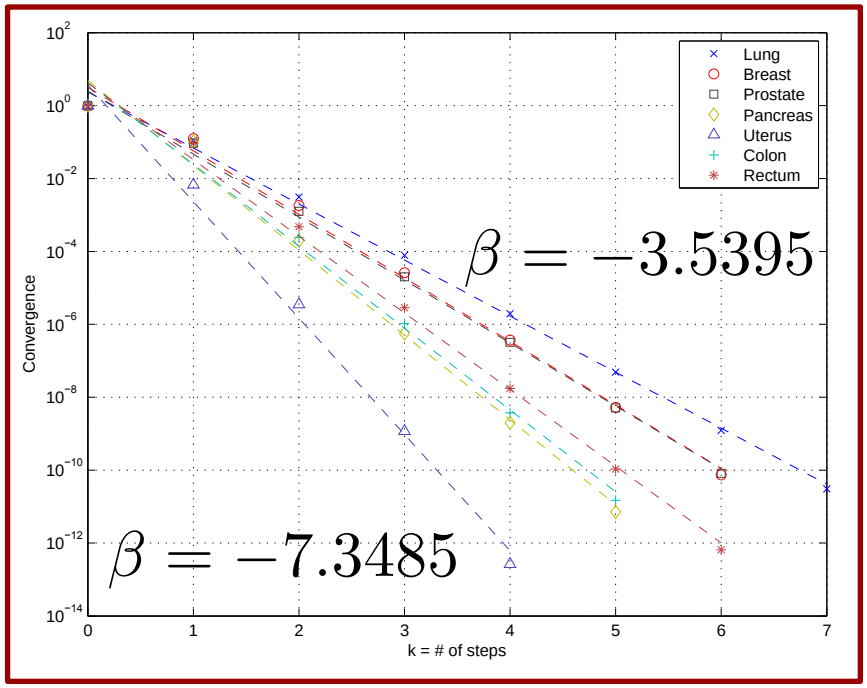

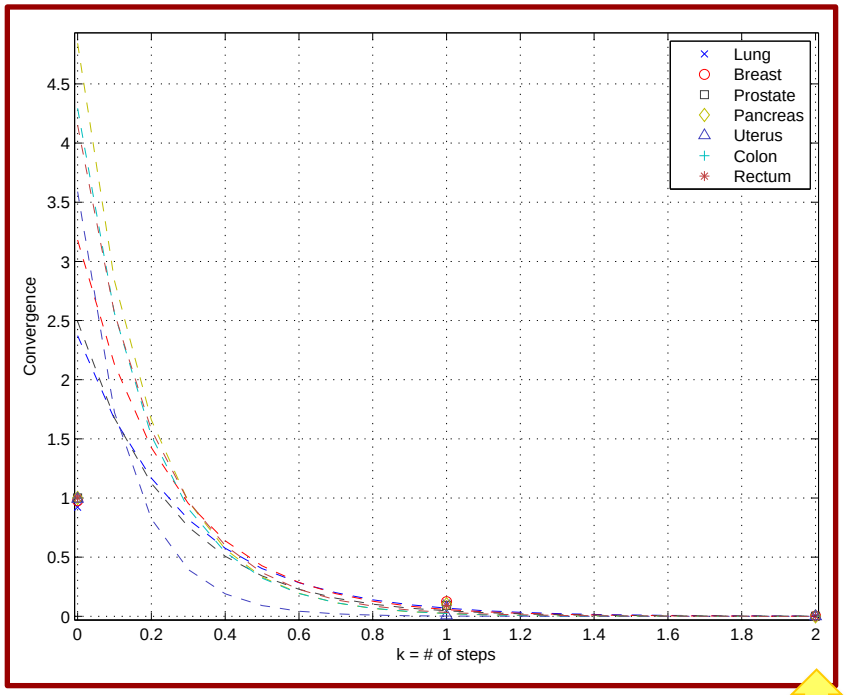

$$\|\vec{v}_k - \vec{v}_\infty\| \sim \alpha \exp(-\beta k)$$

2 steps

Multi-directional pathway diagram: Lung

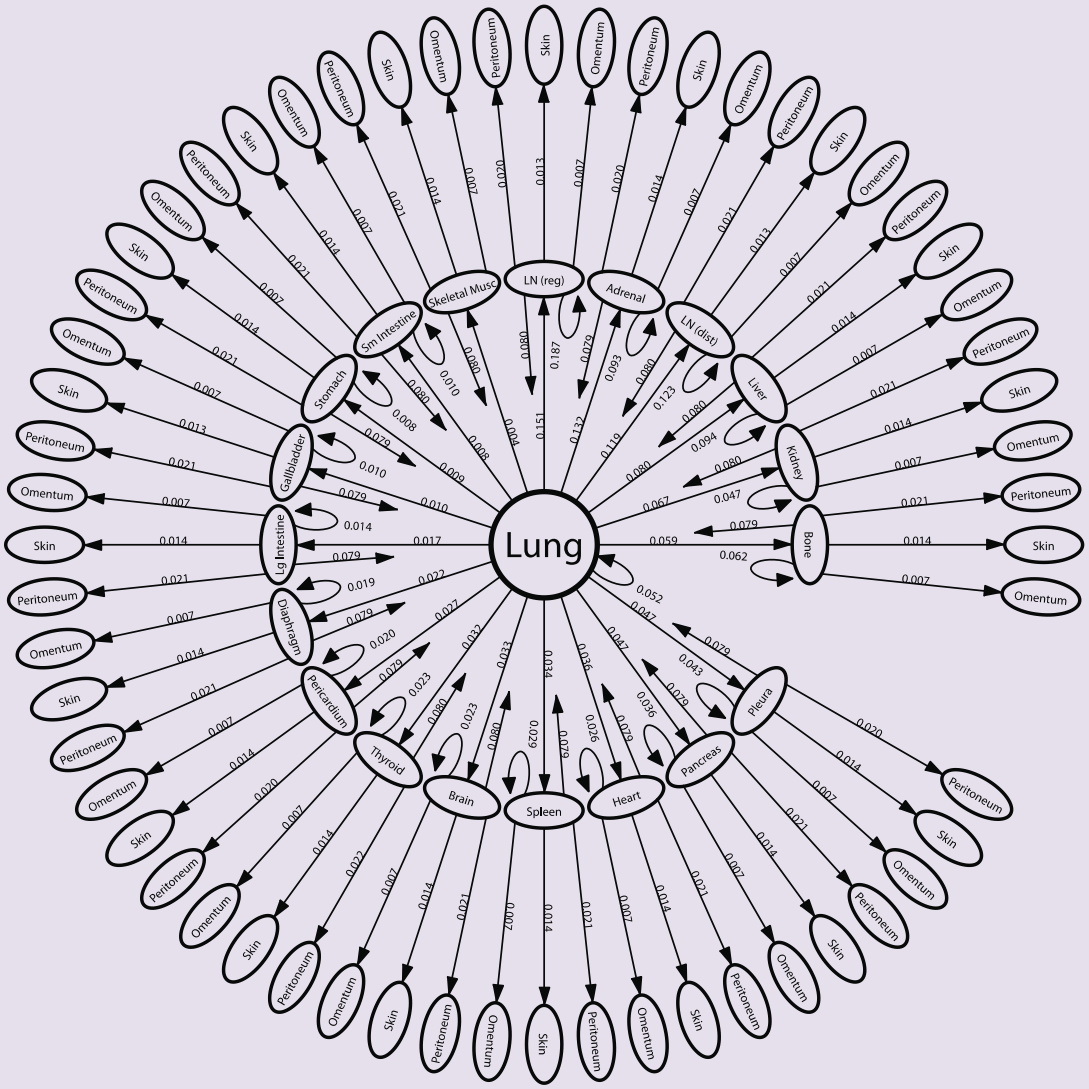

Constructing metastatic pathways

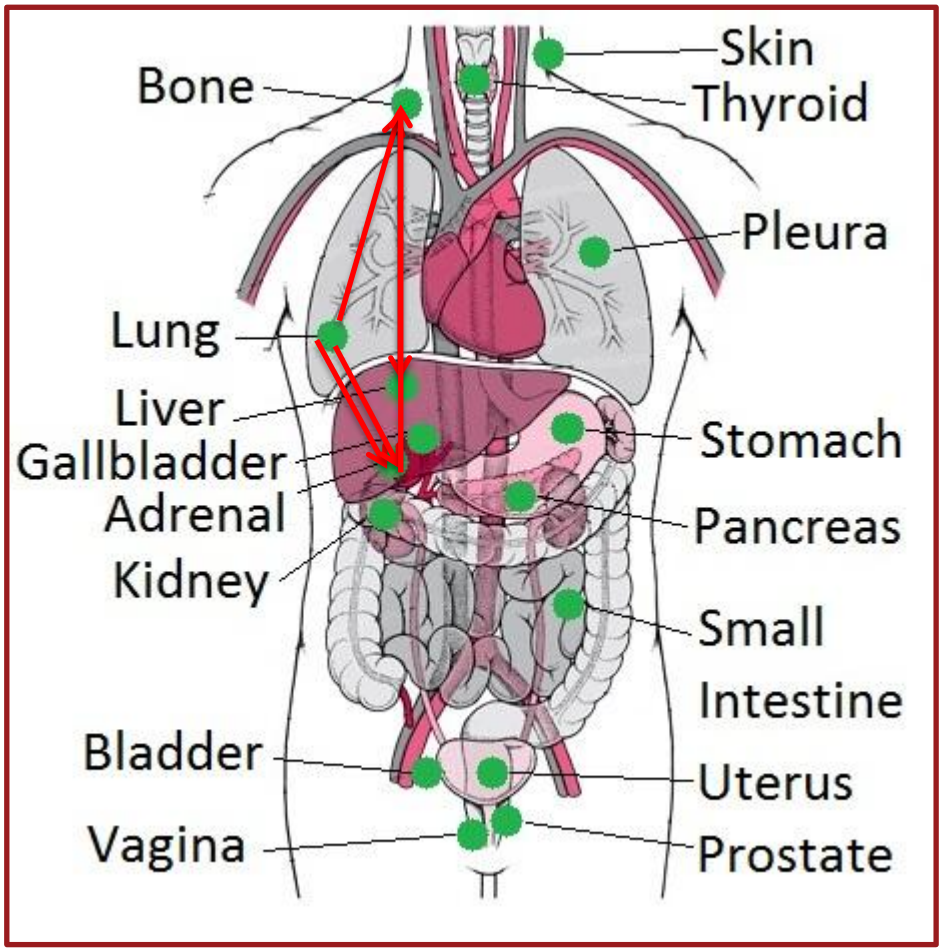

The metastatic pathways

Lung → Bone → Liver → Deceased

Lung → Adrenal → Deceased

Lung → Adrenal → Bone → Deceased

Etc.

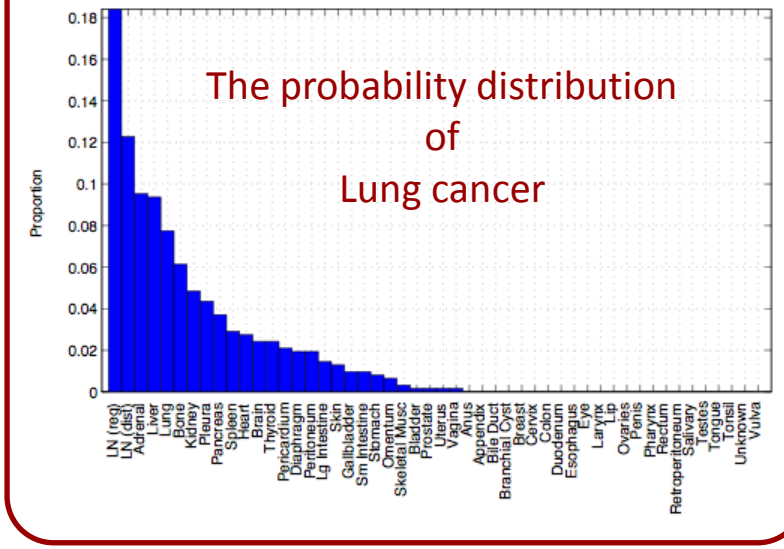

Spreaders & Sponges

Question: Which metastatic sites would make the best `targets' for therapy ?

Metastatic site as spreader or sponge

Spreader: $P_{out}/P_{in} > 1$

Sponge: $P_{out}/P_{in} < 1$

The spreaders and sponges

Reduced order models

Spreaders

Sponges

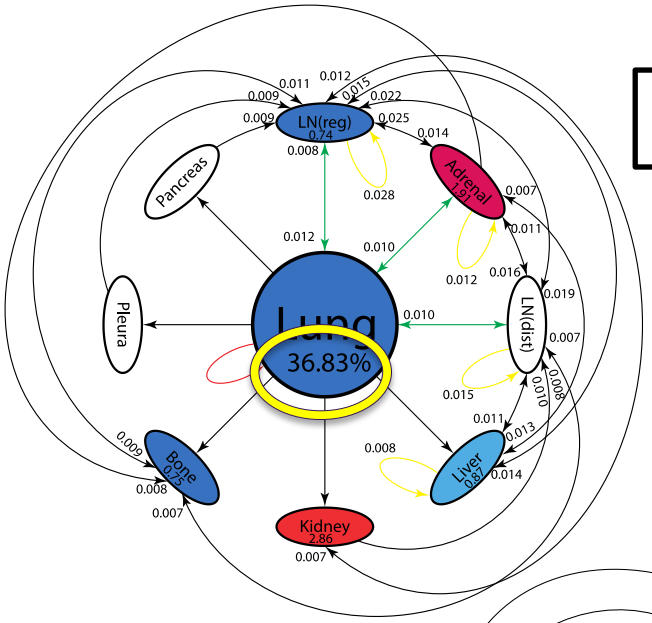

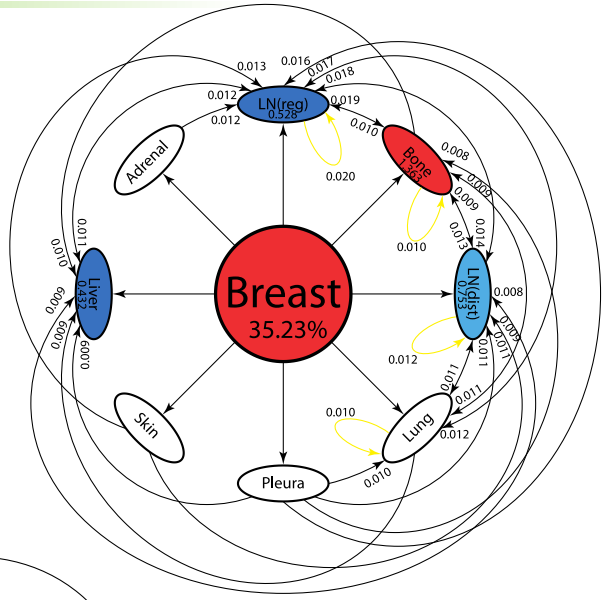

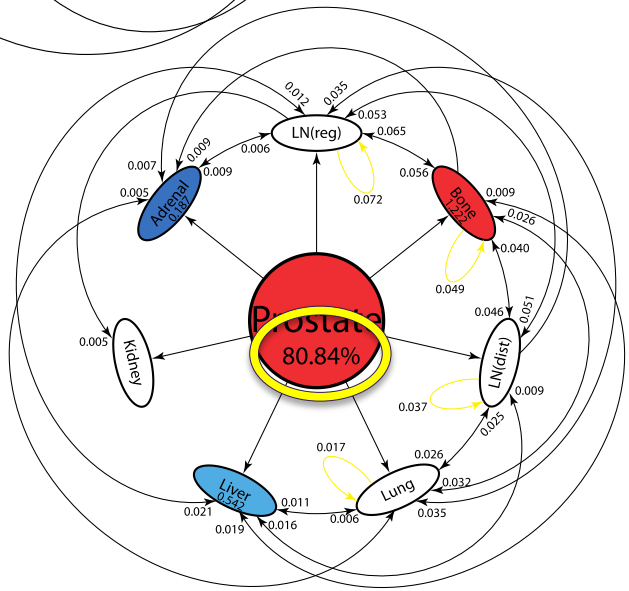

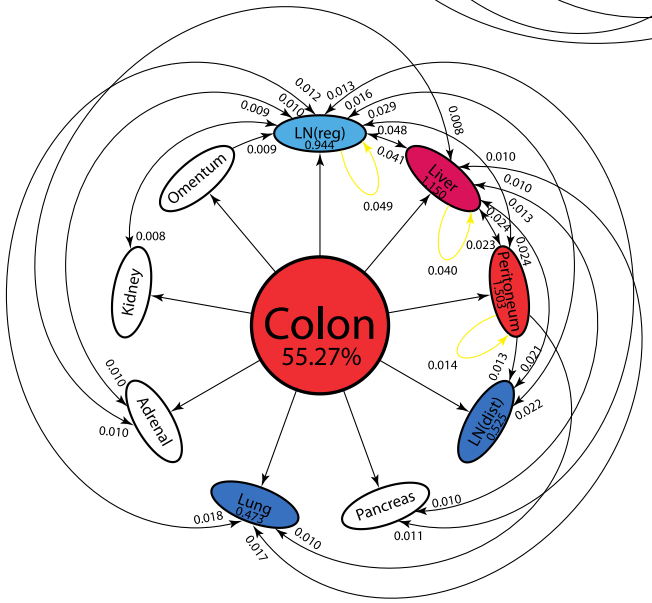

Spreader diagrams

Lung → Adrenal

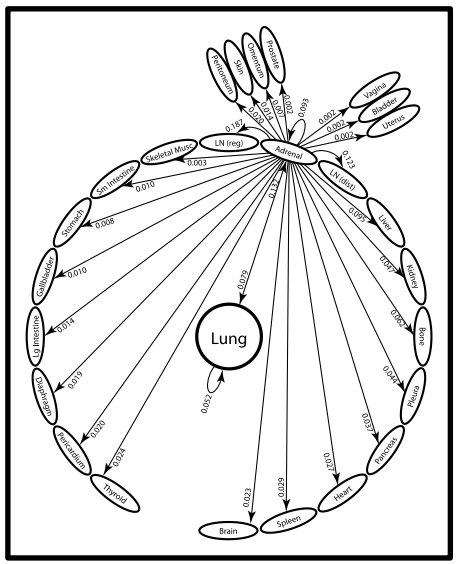

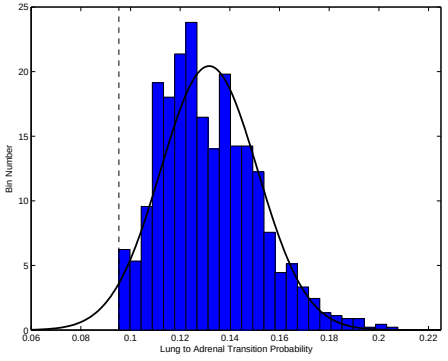

0.132 +/- 0.002

Prostate → Bone

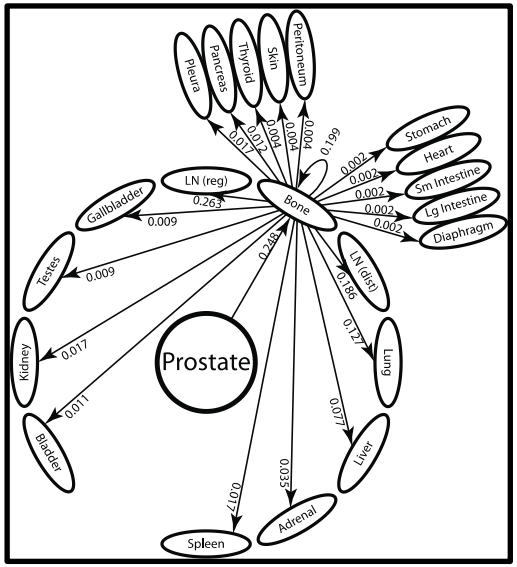

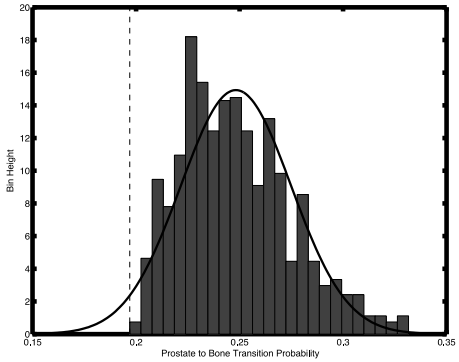

0.248 +/- 0.027

Breast → Bone

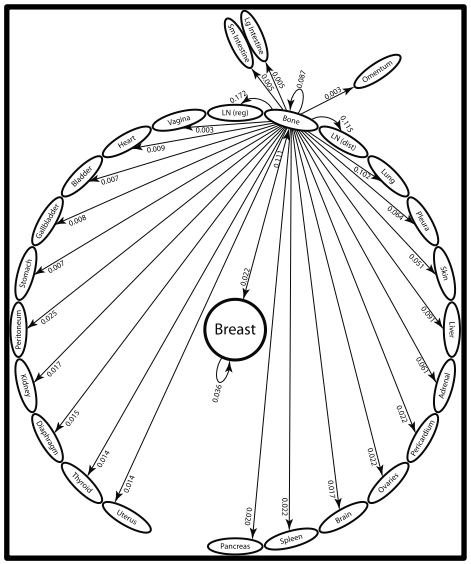

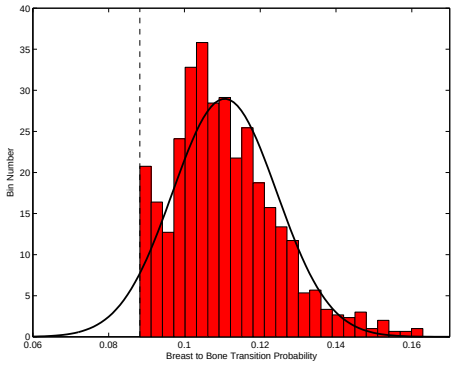

0.111 +/- 0.014

Colon → Liver

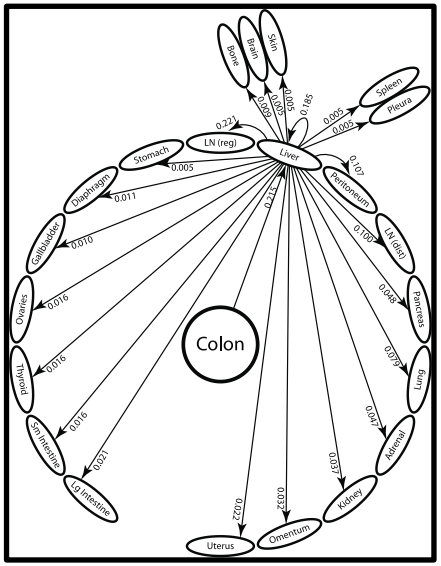

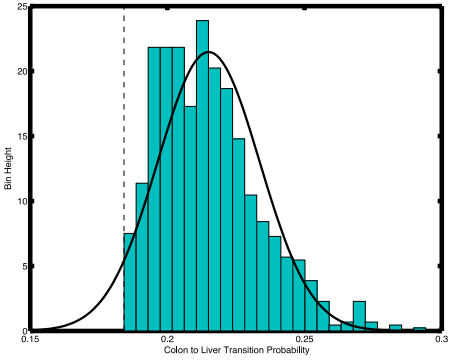

0.215 +/- 0.019

Targeting the spreaders

Question: What would be the response if we could therapeutically target the spreaders?

Spreader → Absorbing state

Entropy decrease, mfpt increase

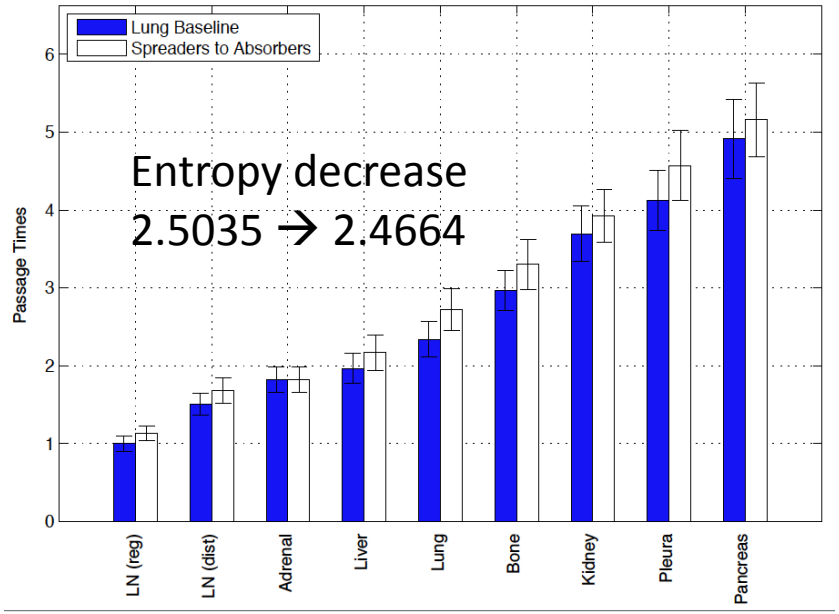

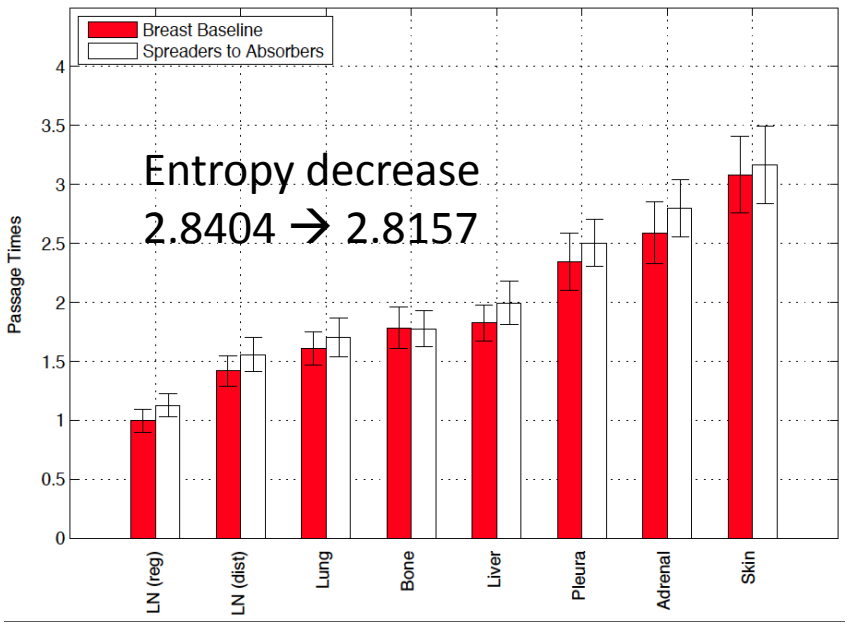

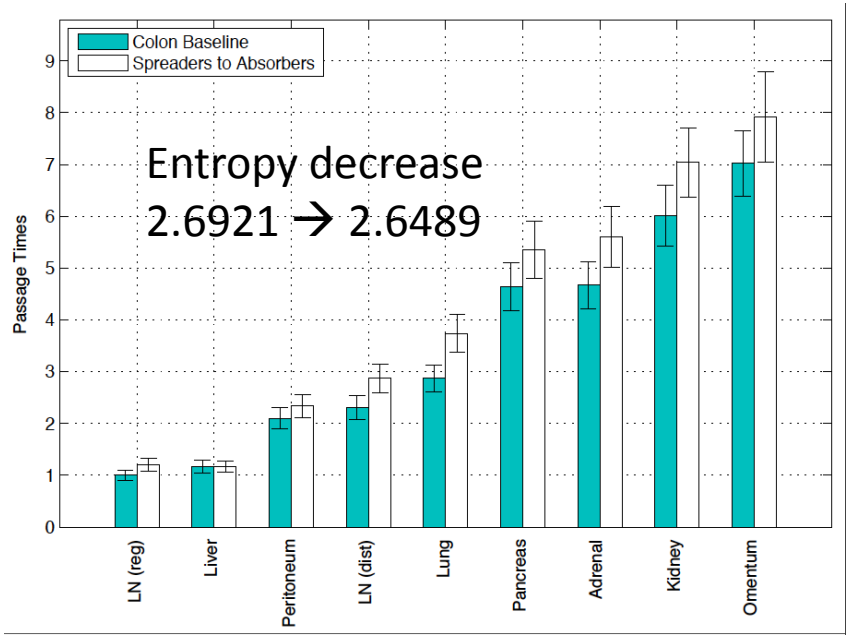

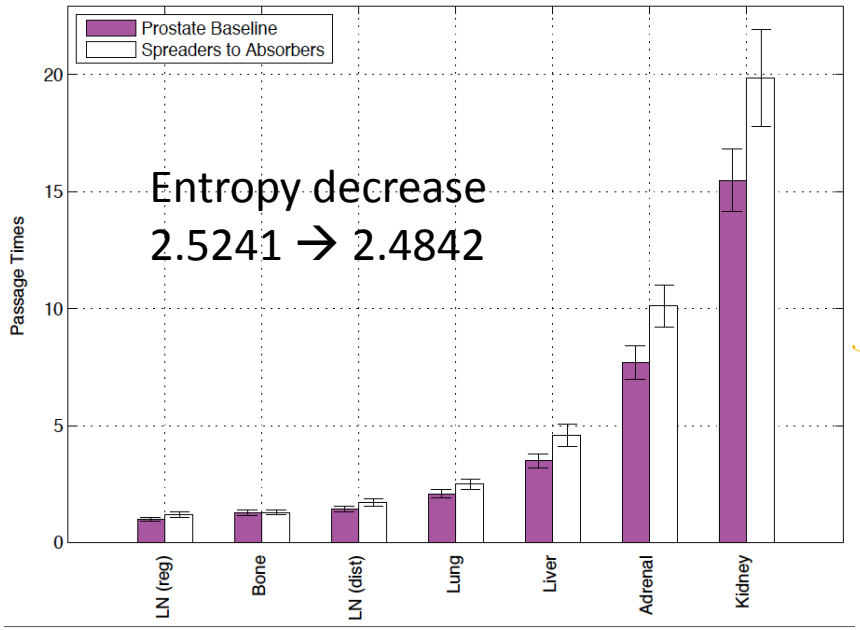

3. CFD models of procoagulant CTCs in the bloodstream

- Cancer patients have a higher than average incidence of blood clot formation leading to stroke.

- CTCs express TF that triggers a complex chain of chemical reactions leading to thrombosis.

Experiment of fibrin formation

Coagulation process of fibrin formation by SW480 cell (McCarty Lab, OHSU)

Cell is ~12 um
60x real time
DIC microscopy

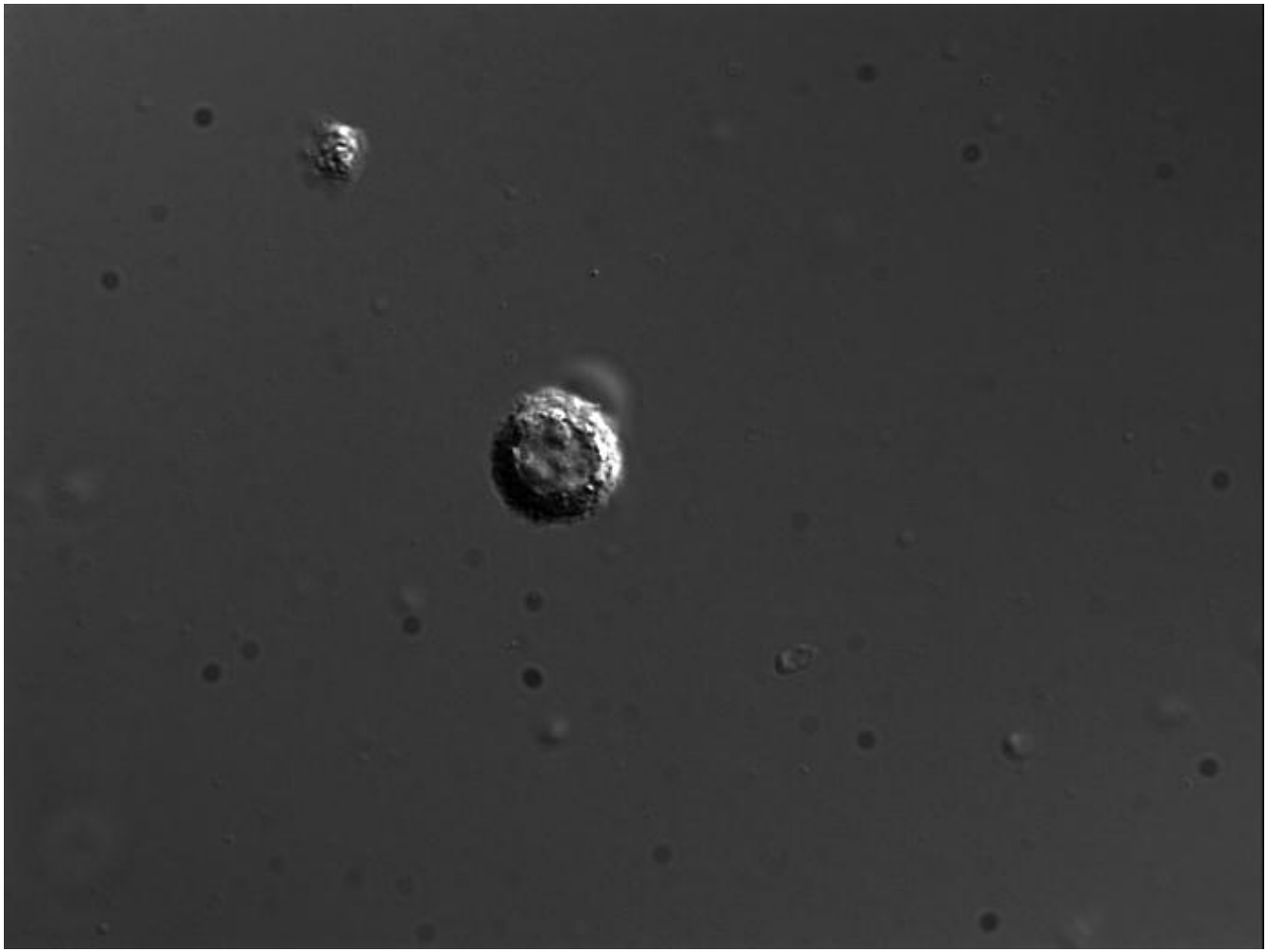

Mathematical infrastructure

Blood flow velocity field

$$\nabla \cdot \vec{u} = 0$$

$$\rho\left(\frac{\partial \vec{u}}{\partial t} + \vec{u} \cdot \nabla \vec{u}\right) = -\nabla p + \mu \Delta \vec{u}$$

$$\vec{u}(\vec{x}, 0) = \vec{f}(\vec{x})$$

Boundary conditions

$$\left.\frac{\partial C}{\partial n}\right|_{\text{wall,cell}} = 0$$

$$\left.\vec{u}\right|_{\text{wall}} = 0$$

$$\left.\vec{u}\right|_{\text{cell}} = \text{velocity of cell boundary}$$

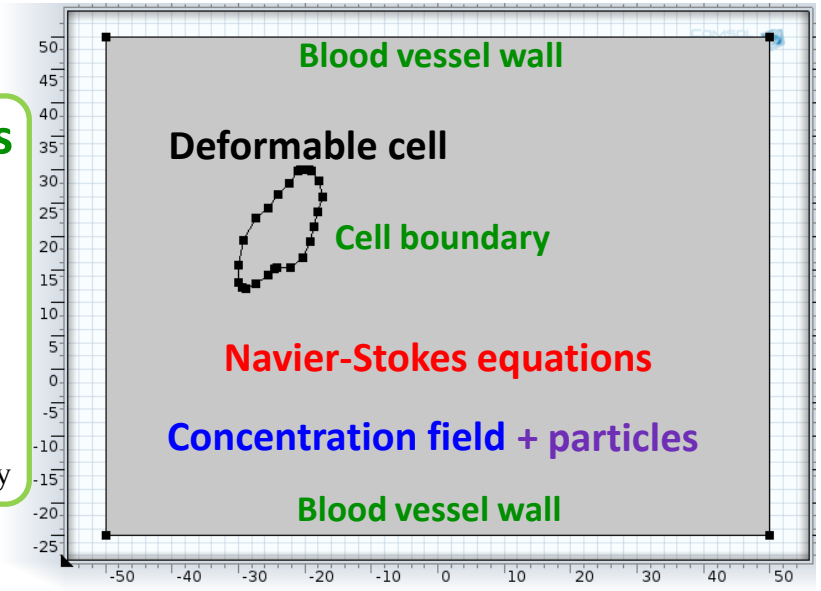

Particles that follow concentration gradients

$$\frac{\partial \vec{q}}{\partial t} = \frac{1}{c_0(C+\epsilon)}\left(\frac{\nabla C}{||\nabla C + \epsilon||}\right)$$

where c_0 is a velocity scaling coefficient

Concentration fields of thrombin associated with each CTC

$$\frac{\partial C^{(i)}}{\partial t} + \vec{u} \cdot \nabla C^{(i)} = \alpha_i \Delta C^{(i)}$$

$\alpha_i (i = 1, \ldots, n)$: Diffusion constants associated with coagulation factors

Blood parameters in venous system

- whole blood: density = 1060 kg/m^3 at 37C
  dynamic viscosity = 3*10^-3 Pa s at 37C
- venules: flow rate: v = 0.03-0.1 cm/s
  diameter: d = 7-50 um

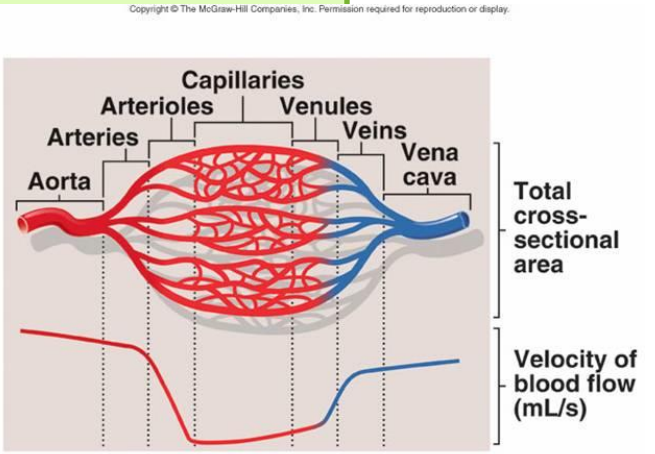

Diffusion coefficients for coagulation factors

Factor	Stokes Radius (nm)	C (nM)	$D^{20,plasma}$ (10^{-7} cm^2 s^{-1})	J/J^{VII}
VII	3.5 (Gladhaug et al. 1970)	7-13 (Fair 1983)	5.1	1
IX	4.1 (Suomela 1976)	40-142 (Yang 1978)*	4.4	3-22
VIII	8.8 (Hoyer et al. 1981)	0.4-1 (Hoyer 1994)*	2	<<1
X		101-162 (Epstein 1984)	5	8-23
V	9.5 (Esmon 1979)	12-42 (Kamphuisen 2000)	1.9	2-10
II	4.1 (Stenflo 1972)	1200-1730 (Legnani 2003)	4.4	100-266

* calculated (FIX: 100% = 4.5 μg mL^{-1}; FVIII: 100% = 0.2 μg mL^{-1})

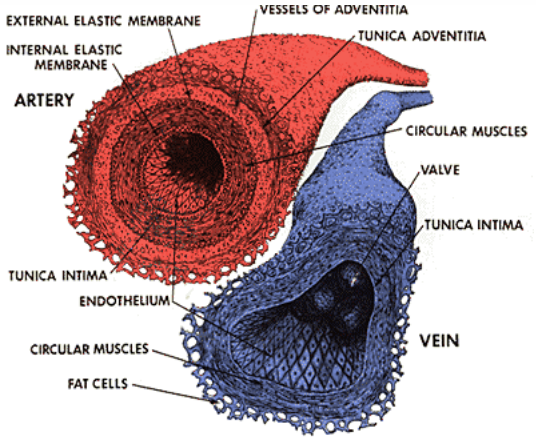

CFD model of flow in channel

Breast cancer cell imaged from Kuhn Lab

DIC image

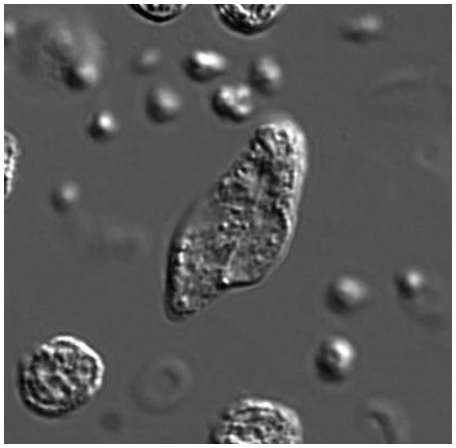

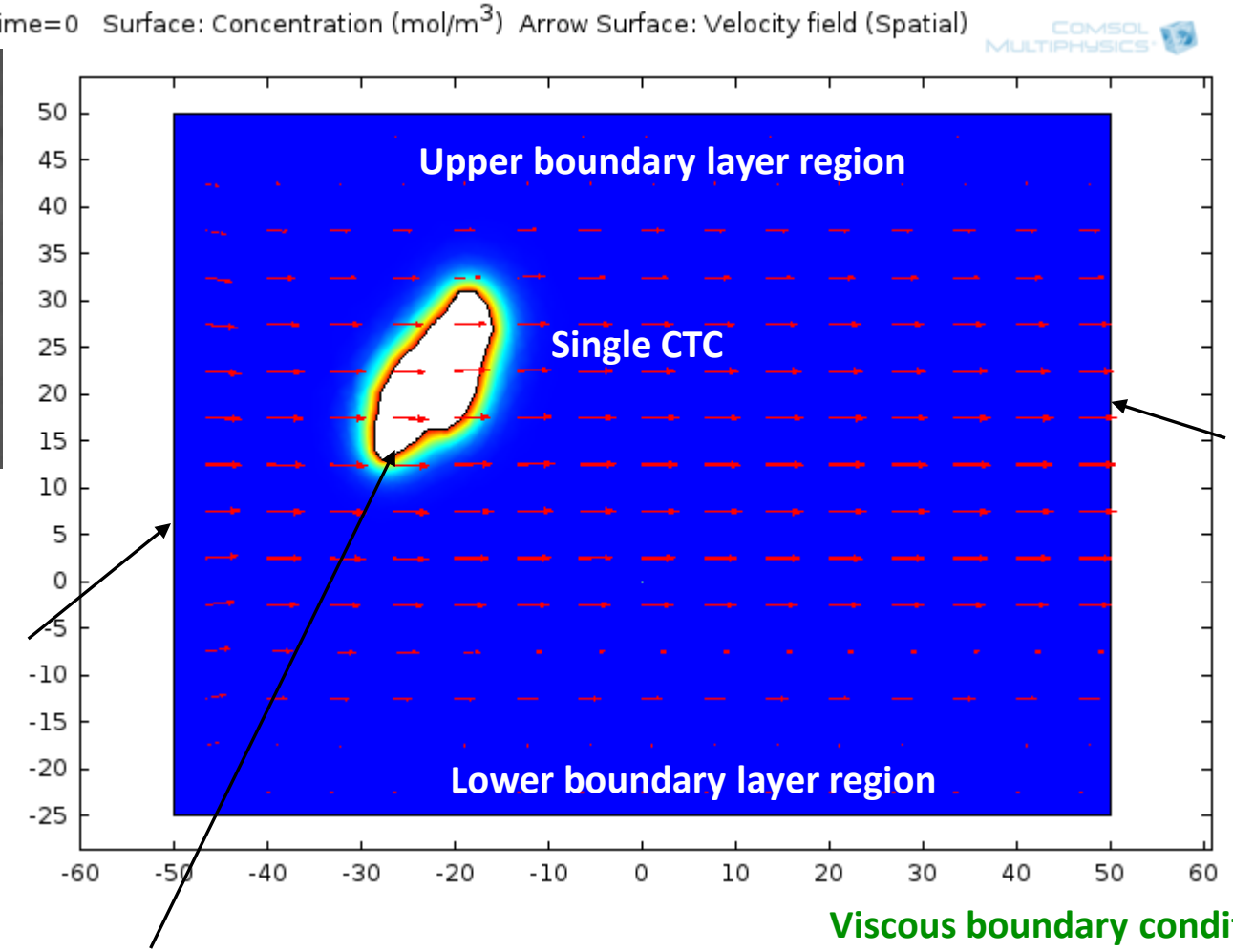

Outflow

Inflow (flow profile set up by pressure gradient)

Concentration field of thrombin on surface of CTC

Viscous boundary conditions along vessel walls

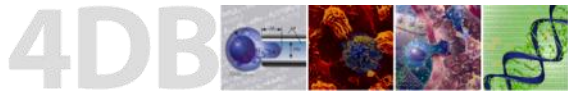

Simulation of CTC under flow

Blood velocity field

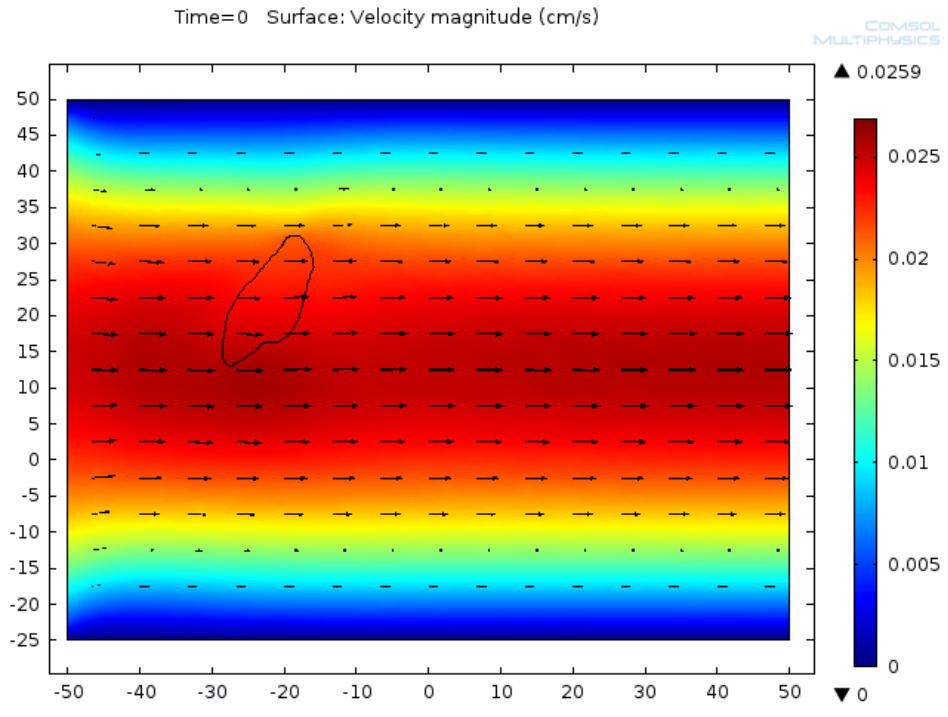

Thrombin concentration field

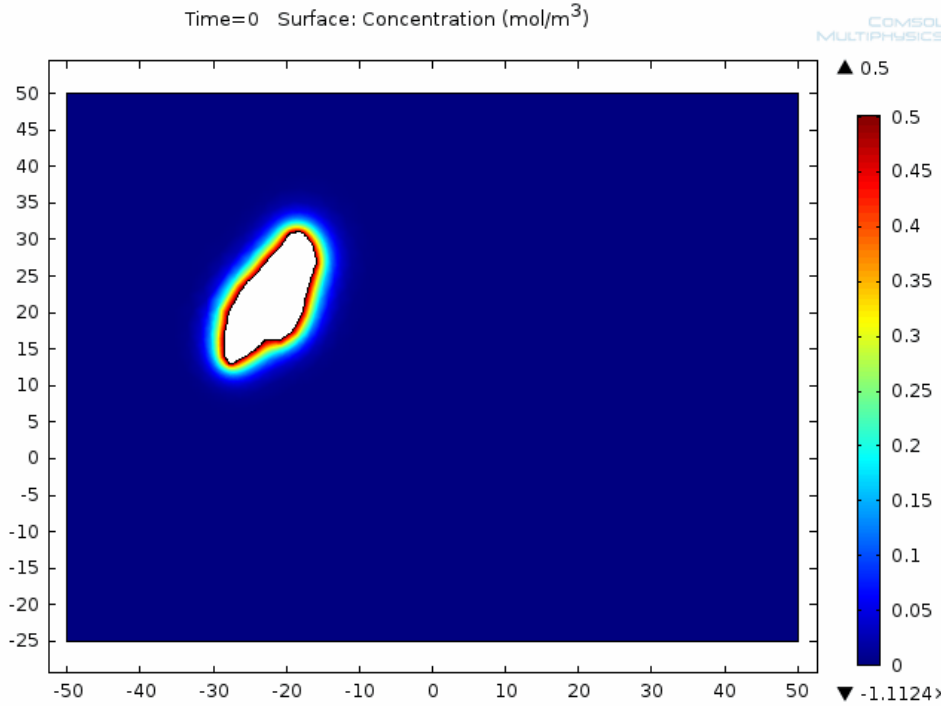

Max velocity = 0.026 cm/s

Diffusion coefficient = 1e-7 cm^2/s

Simulation of CTC under flow

Thrombin field and velocity vectors

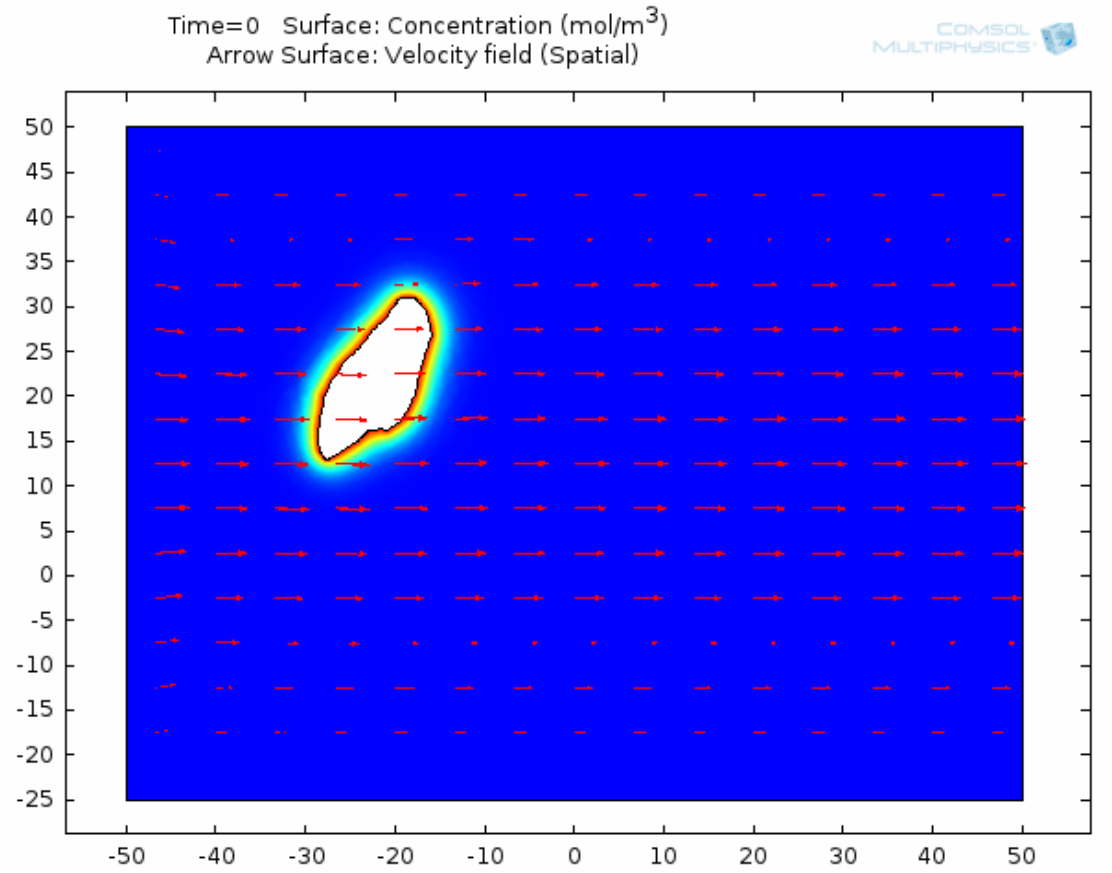

Adaptive mesh generation

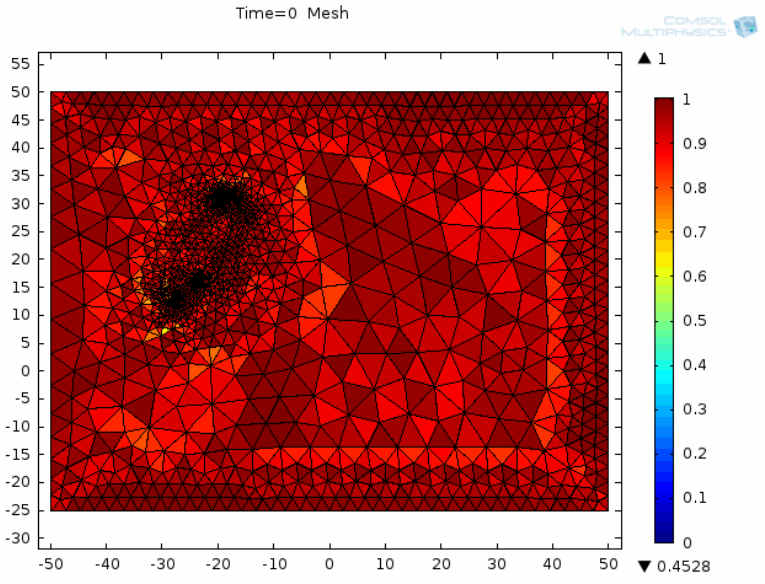

Complete mesh consists of 2552 domain elements and 183 boundary elements

CFD model of branching venules

DIC image

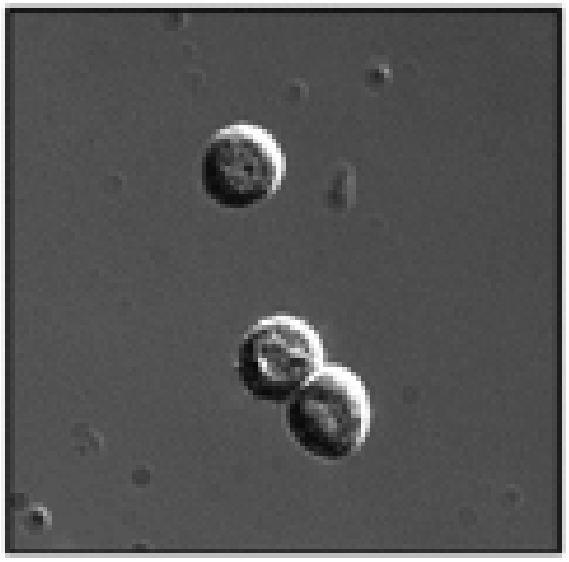

SW480 colon adenocarcinoma cells

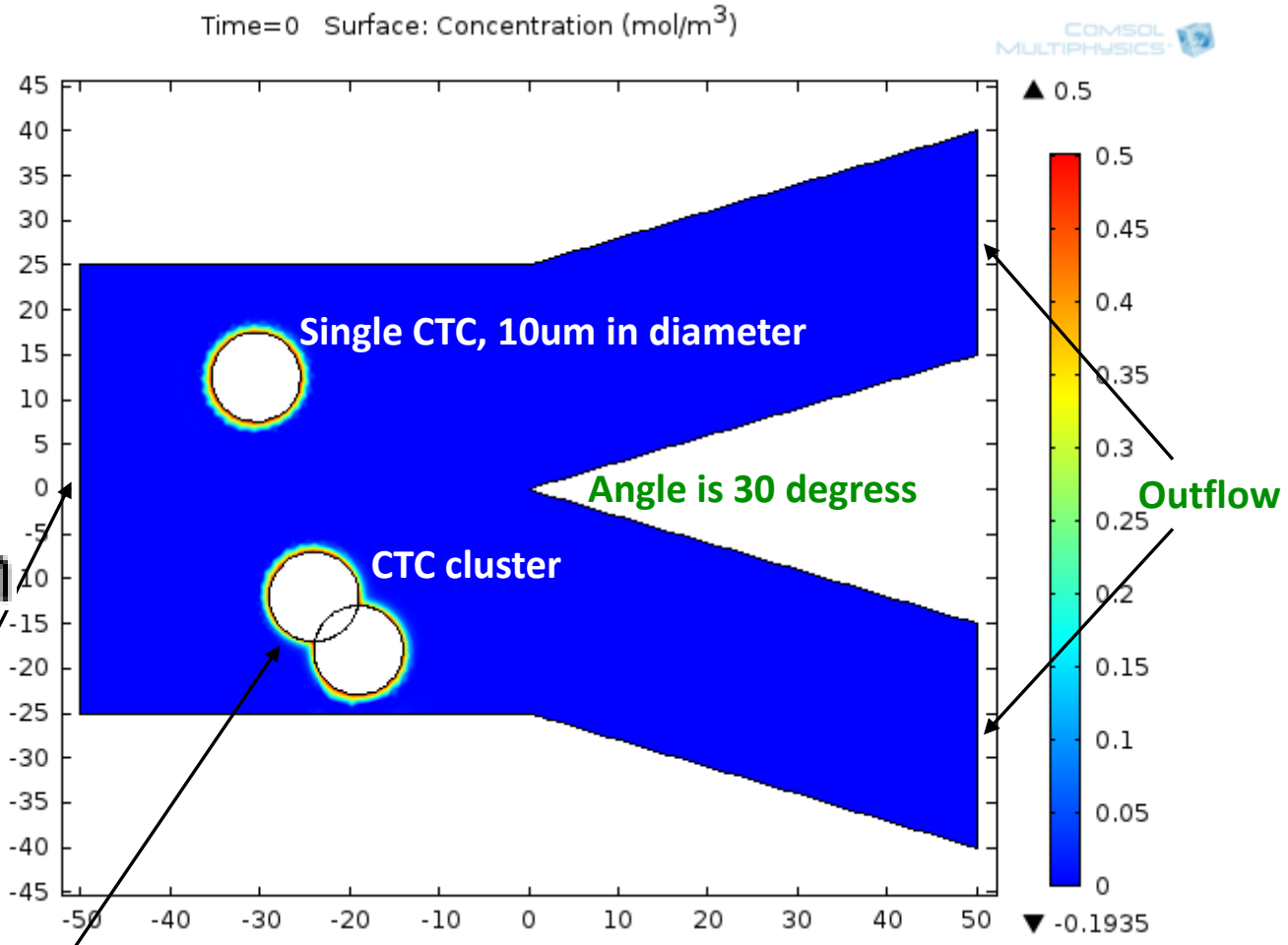

Simulation of CTC cluster under flow

Blood velocity field

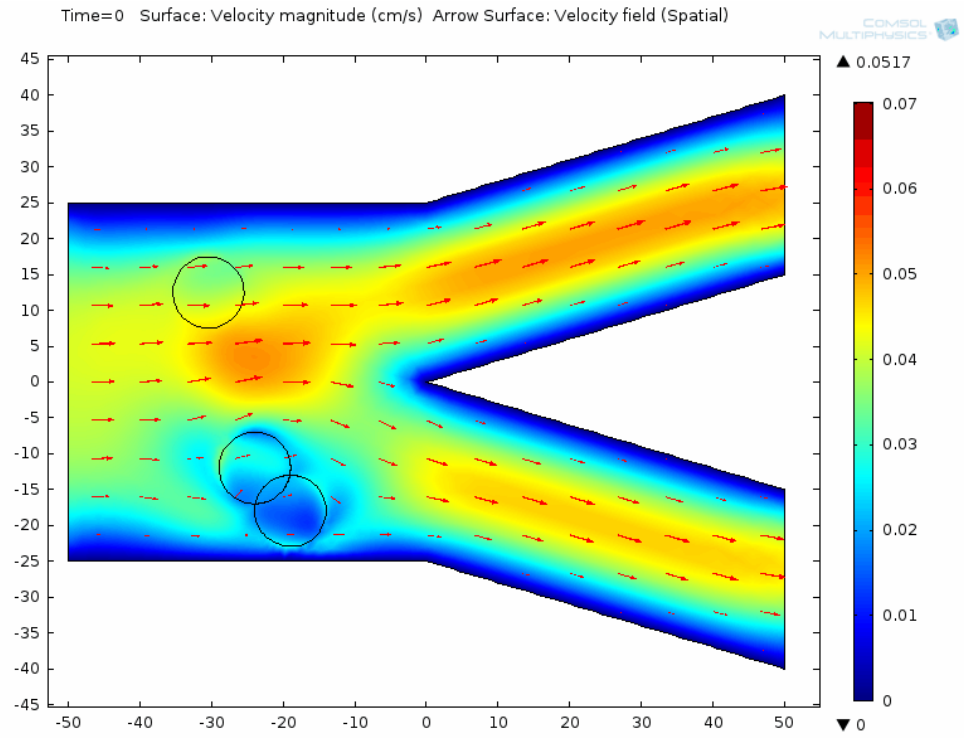

Thrombin concentration field

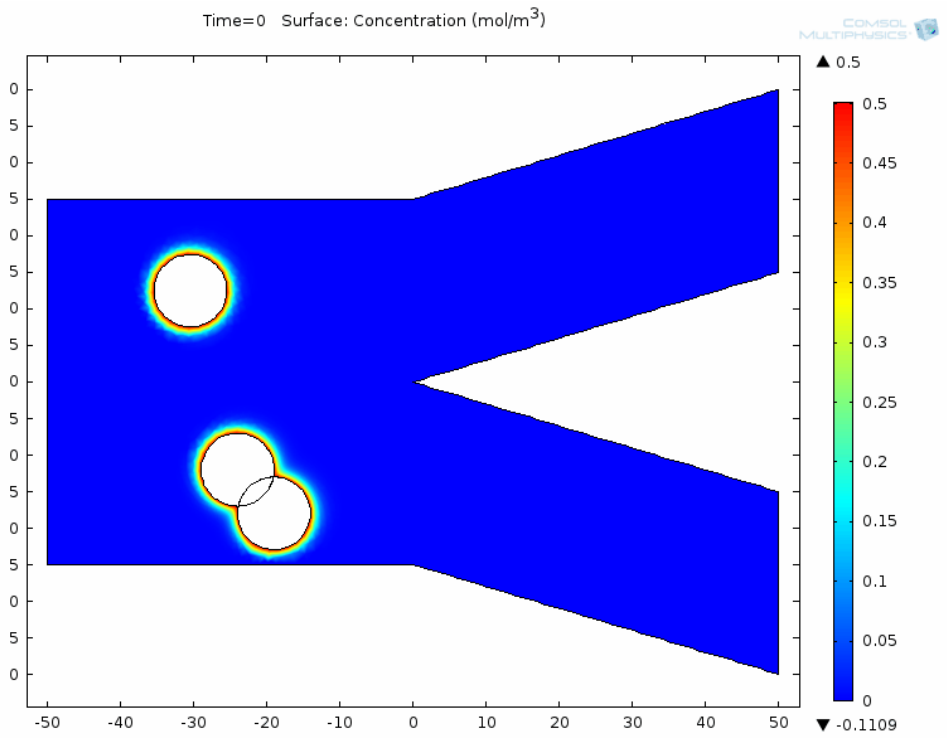

Max velocity = 0.08 cm/s

Diffusion coefficient = 3e-7 cm^2/s

Simulation of CTC cluster under flow

Particle tracking for thrombin field

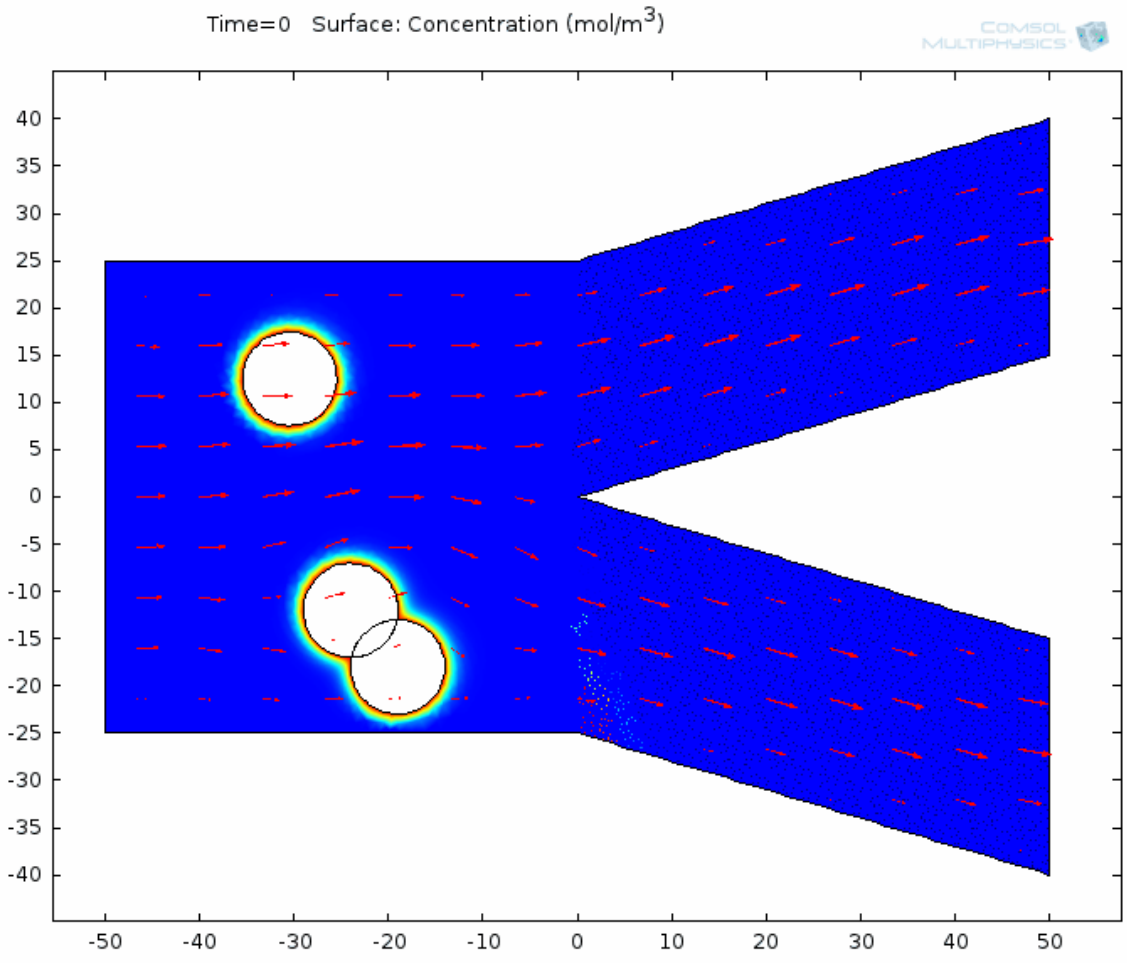

1500 particles in simulation

Adaptive mesh generation

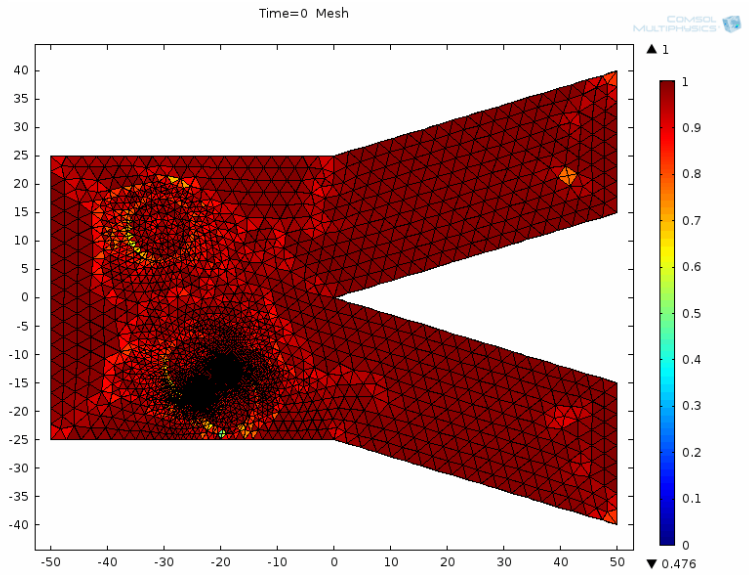

Complete mesh consists of 5696 domain elements and 334 boundary elements

Patient sample to computational simulation

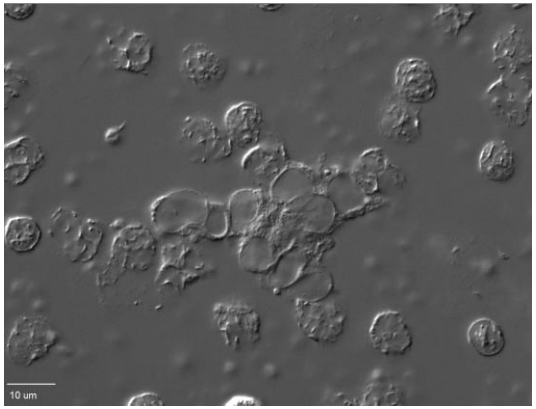

(a) DIC image of lung cancer cluster.

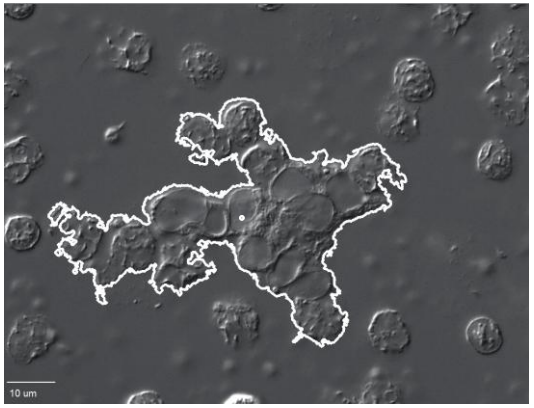

(b) Outline of cluster is obtained using Cell Profiler. Center of cluster is marked by white dot.

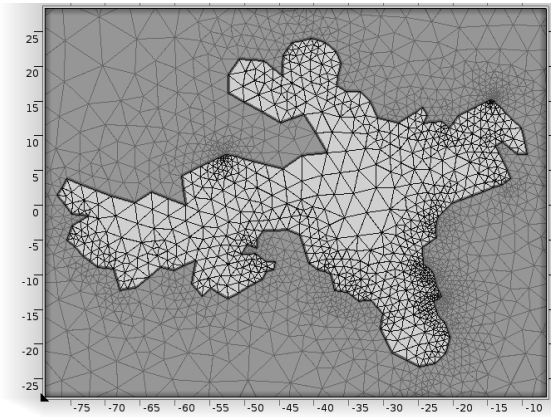

(c) Shape of cluster is generated in computational domain (COMSOL).

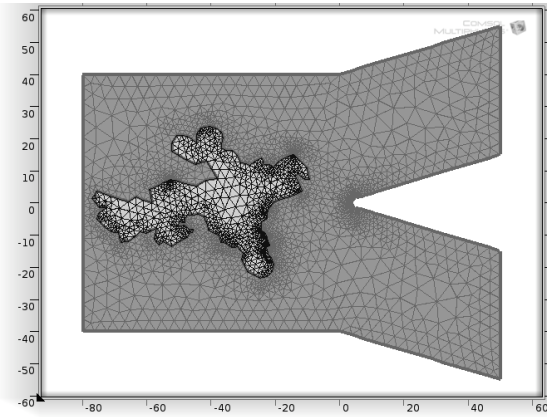

(d) Cluster is placed in a branching venule, with the cluster centered vertically in the middle of the venule.

Blood velocity field

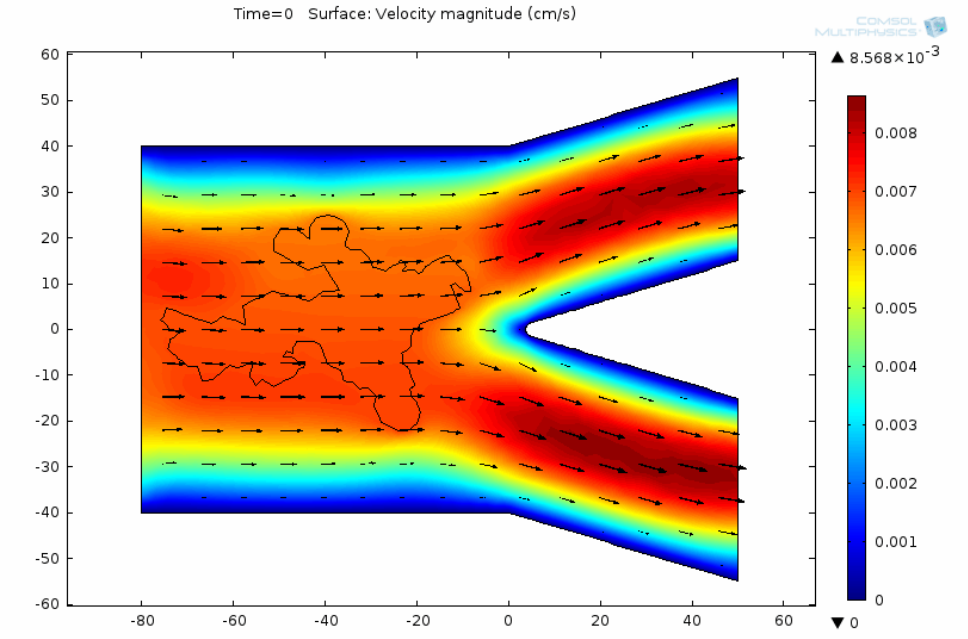

Maximum velocity ~0.008 cm^2/s

Upon reaching the “fork in the vessel”, the cluster begins to deform and significantly obstructs the blood flow.

Mesh generation

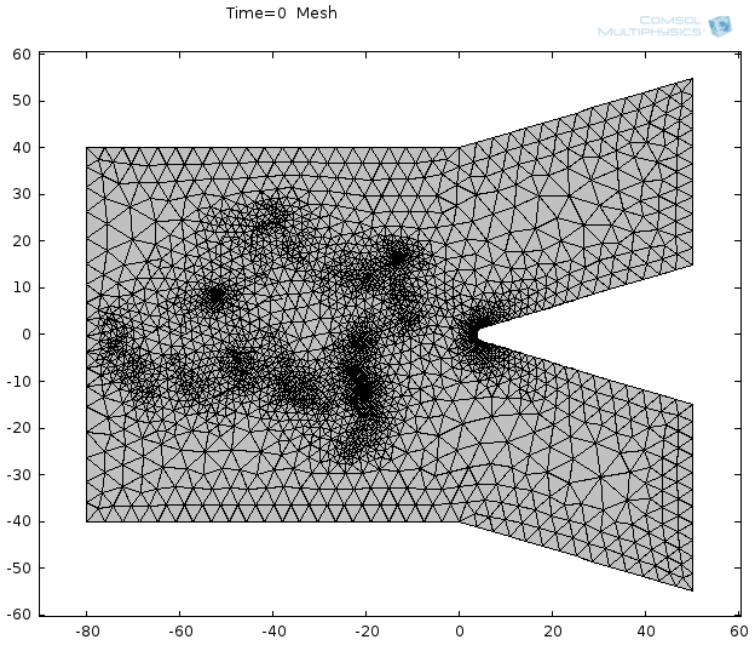

Complete mesh consists of 4872 domain elements and 346 boundary elements.

Concentration field of thrombin

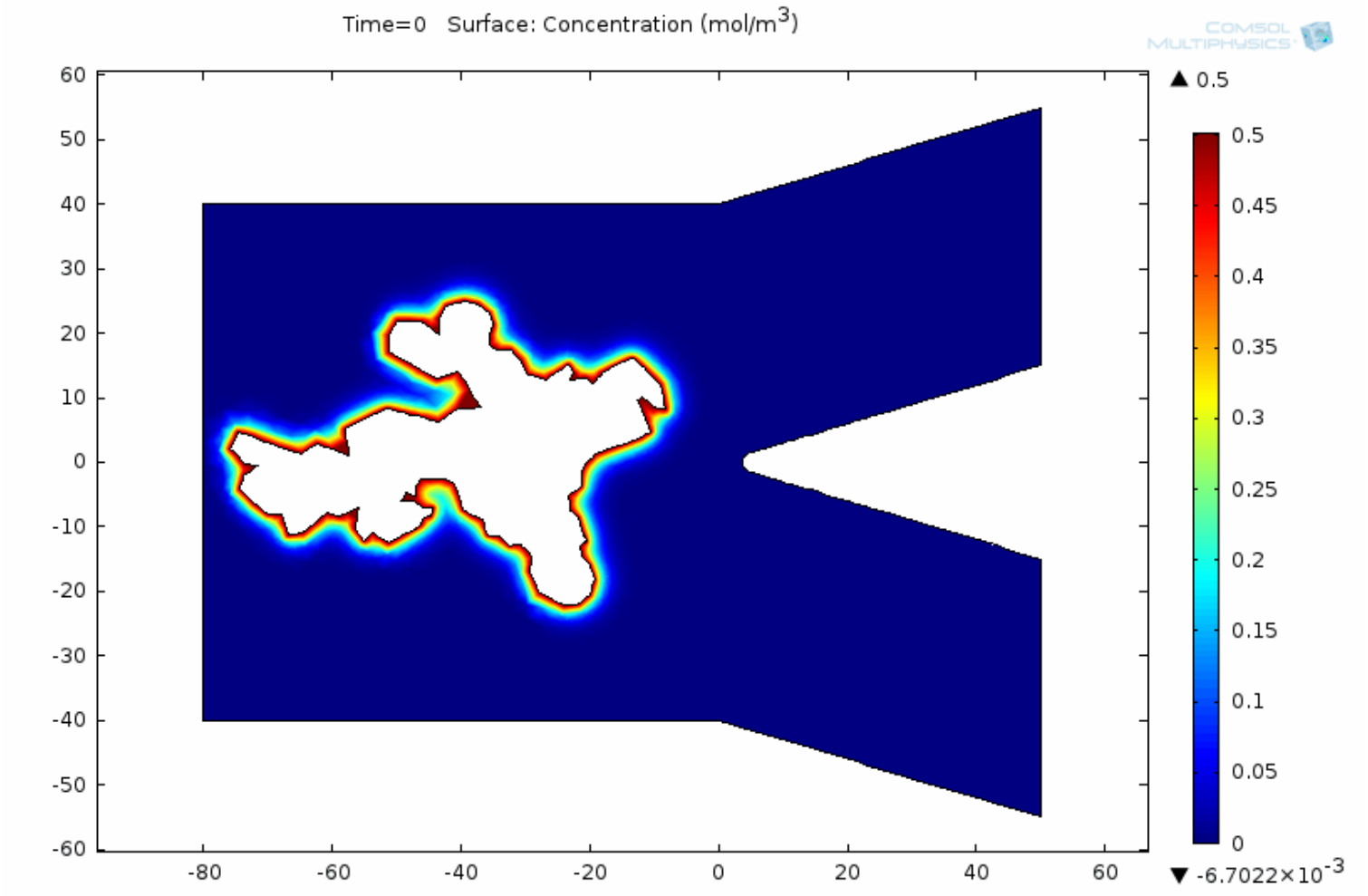

Diffusion coefficient = 1e-7 cm^2/s

Particles are tracking velocity field with concentration field shown

$$\frac{\partial \vec{q}}{\partial t} = \vec{u}$$

1000 particles are released at t = 0 s

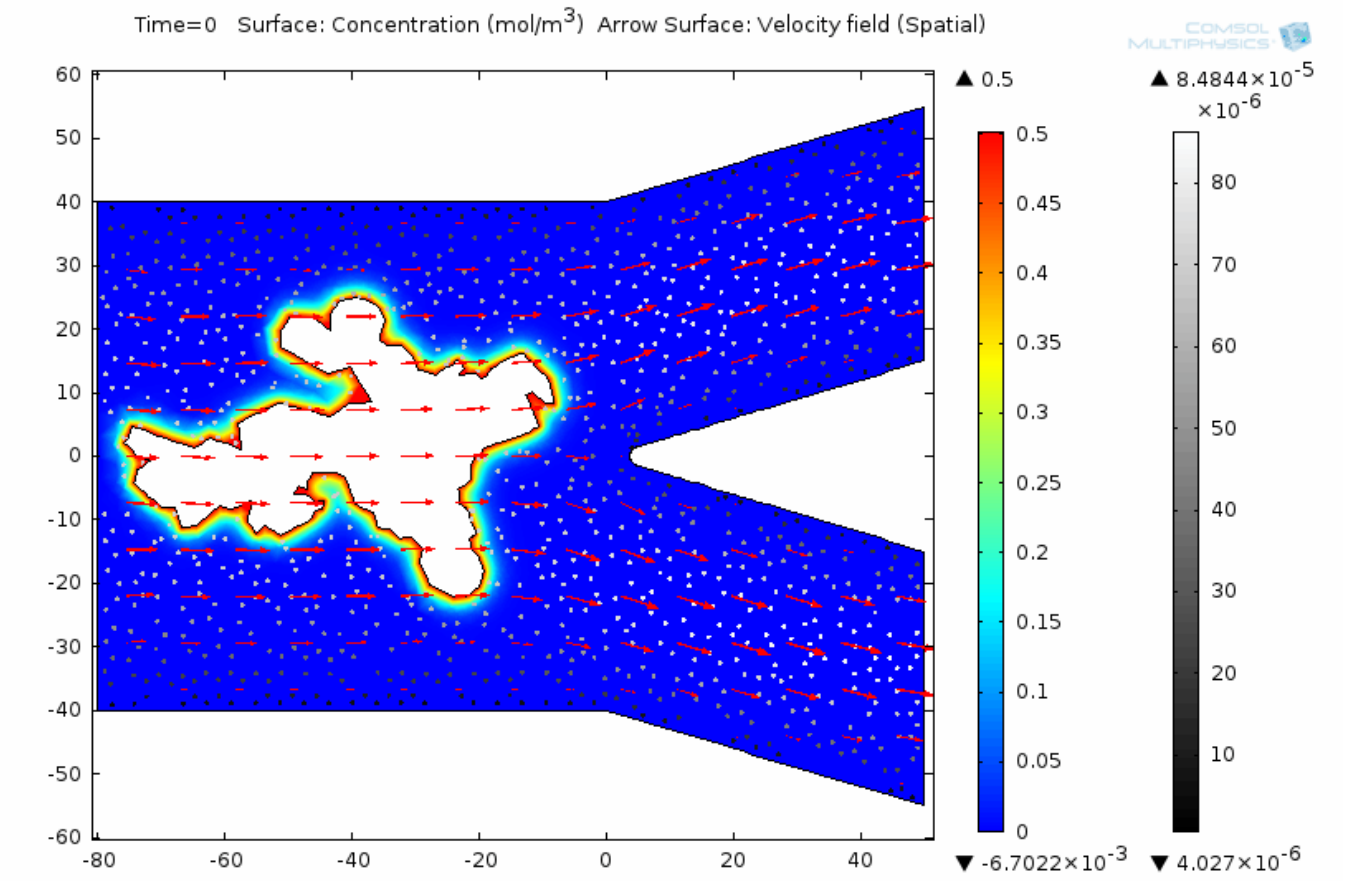

The particles clearly display the parabolic flow profile of the blood, and show that blood flow in the lower branch is slightly faster than in the upper branch.

Particles are tracking concentration field

$$\frac{\partial \vec{q}}{\partial t} = \frac{1}{c_0(C+\epsilon)} \left(\frac{\nabla C}{||\nabla C + \epsilon||} \right) \text{where } c_0 \text{ is a velocity scaling coefficient}$$

5000 particles are released four times at t = 0, 0.15, 0.3, 0.45 s

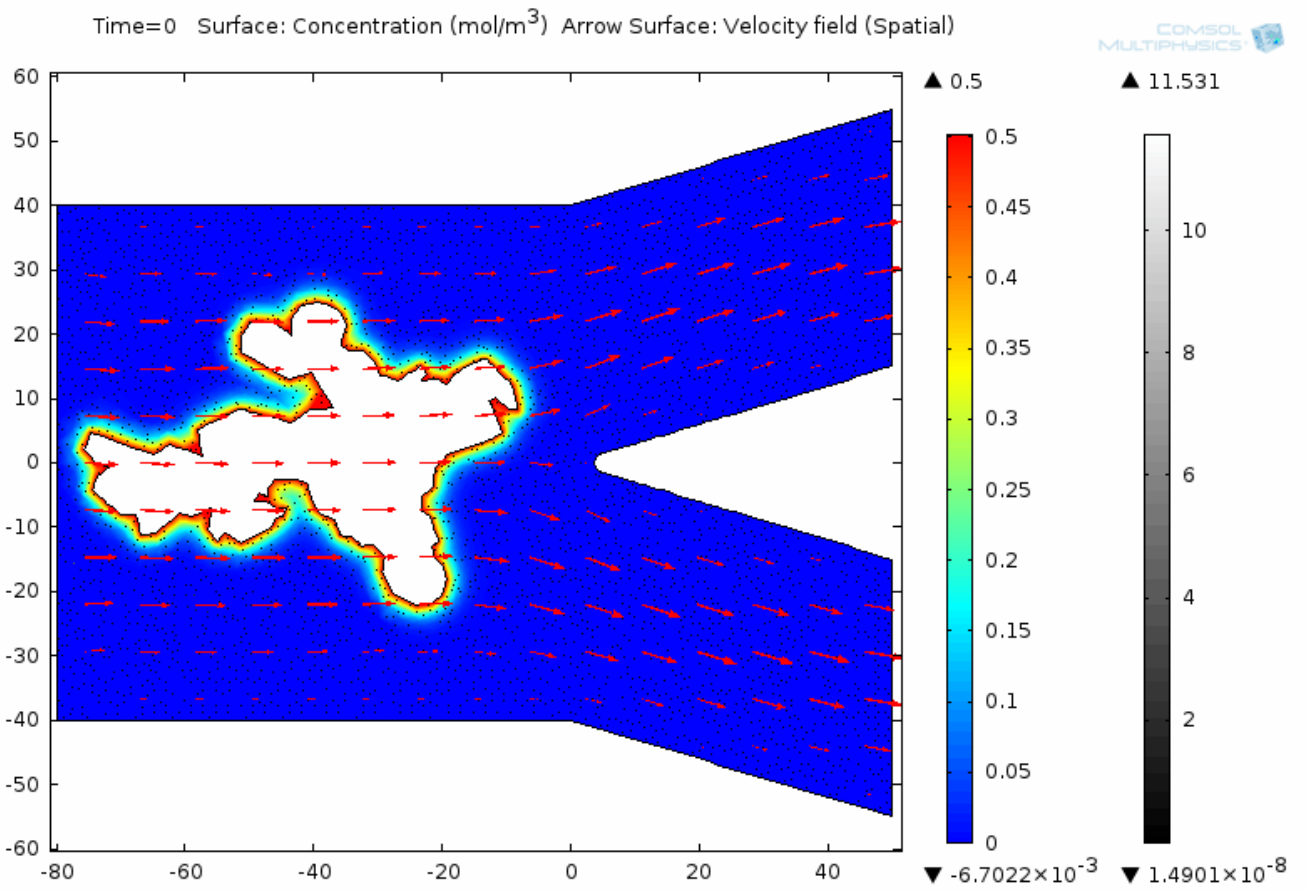

The particles show that early in the simulation, the thrombin field closely resembles the shape of the cluster, whereas later in the simulation, the thrombin field is dictated by the blood vessel geometry.

4. Building low-dimensional deformation models of CTCs using `Active Shape Algorithms'

- Bridging the gap between experiment and computations

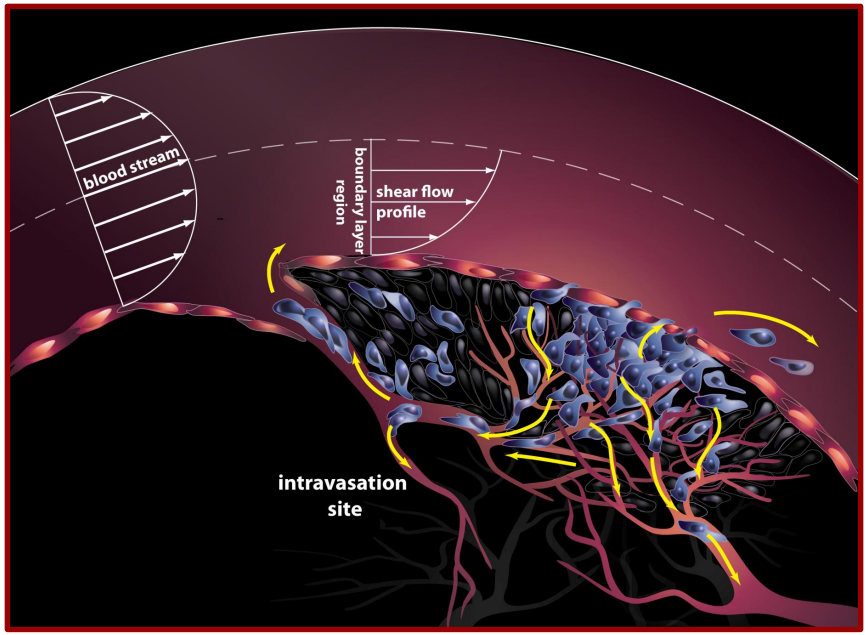

MDA-MB-231 breast cancer cell in flow

(McCarty Lab OHSU)

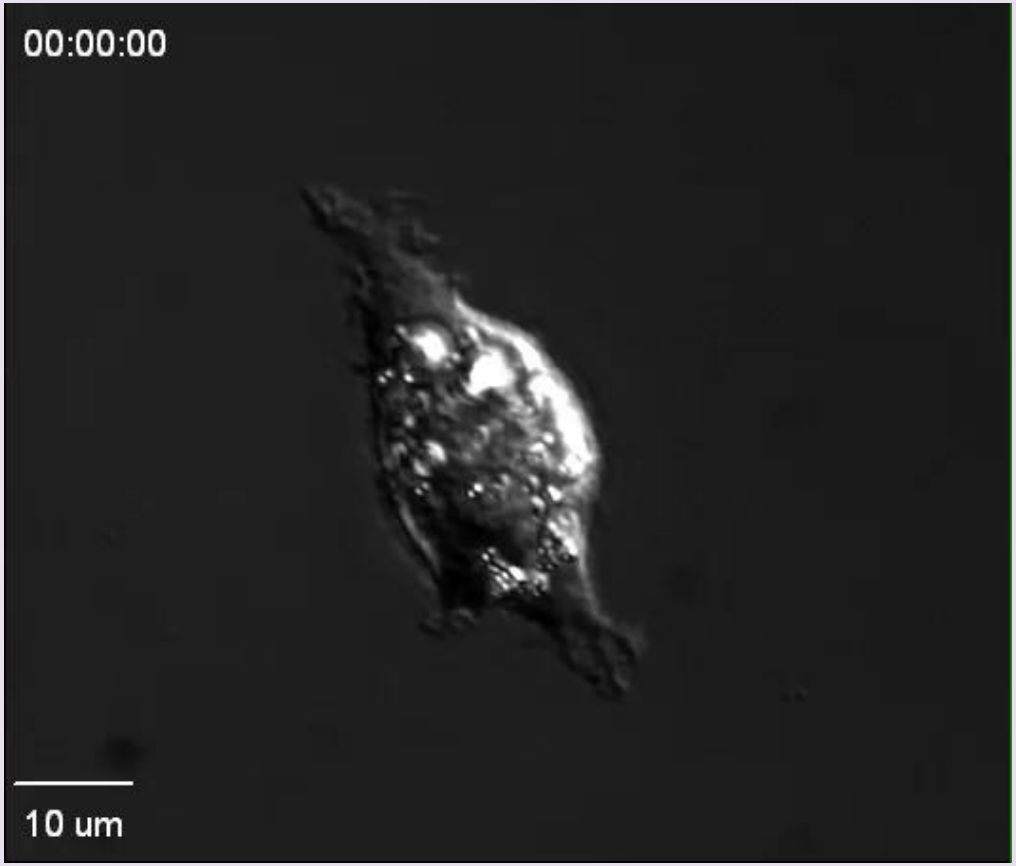

Low-d deformation model of cancer cell release

(McCarty Lab OHSU)

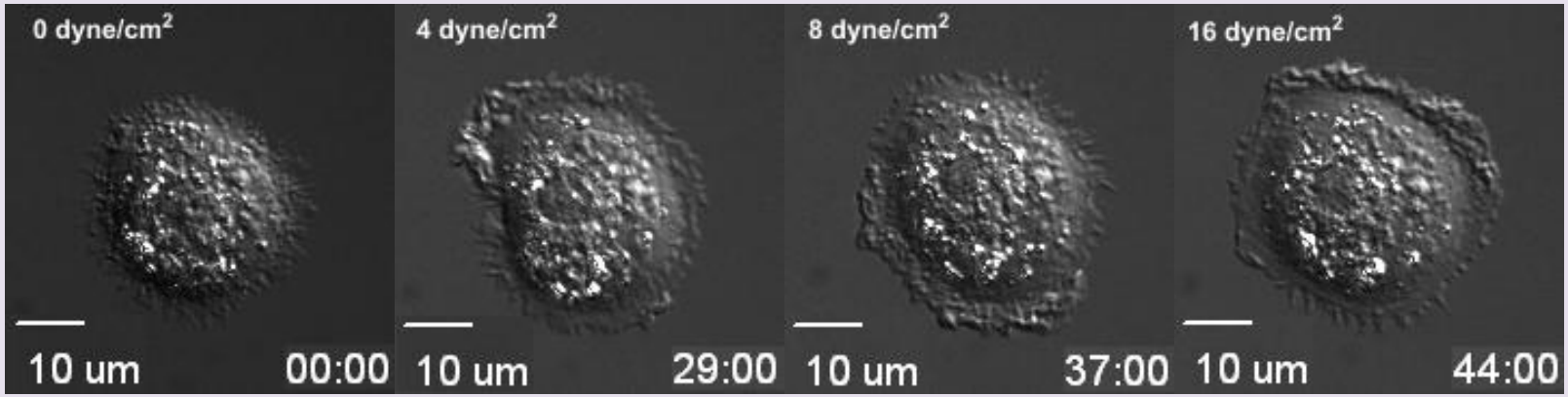

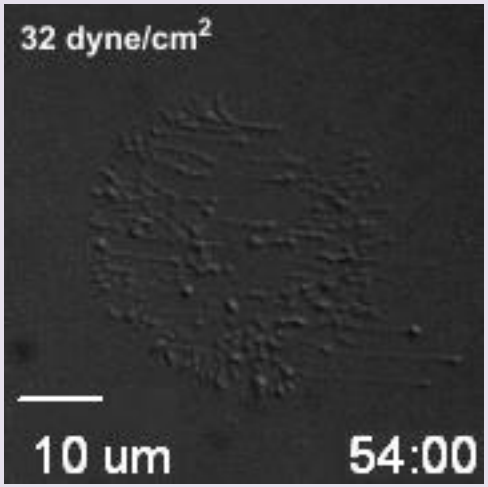

Low-d deformation model of cancer cell release

- Active shape modeling gives principal modes of deformation
- Used to `train' parameters in an `empirical constitutive equation' for a low-dimensional model
- The model is then used in a stochastic Stokes flow simulation of cell release

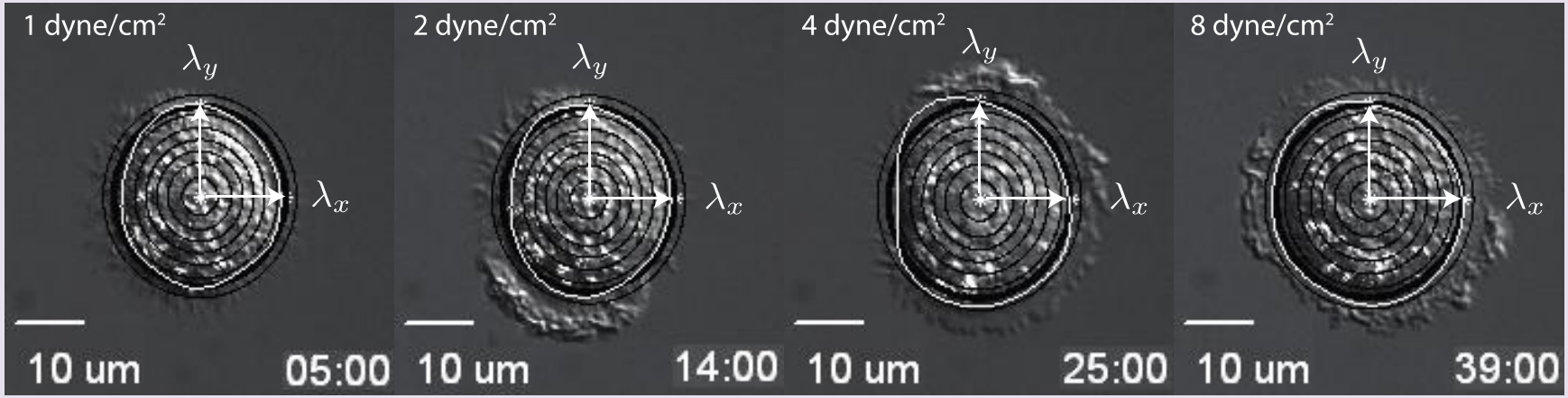

5. Cell-trafficking models based on evolutionary game theory

- Building a dynamical system on the anatomical network that tracks the evolutionary properties of different cell populations

22 anatomical sites for prostate cancer

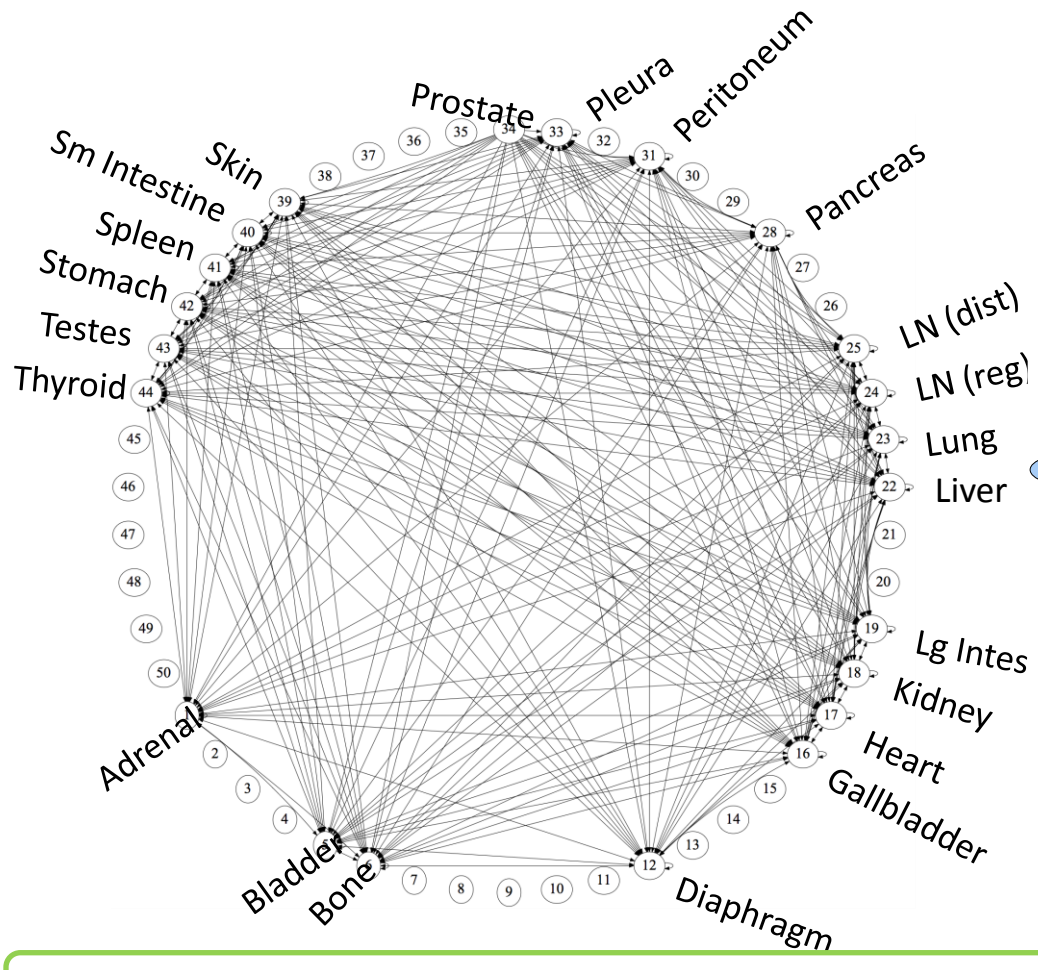

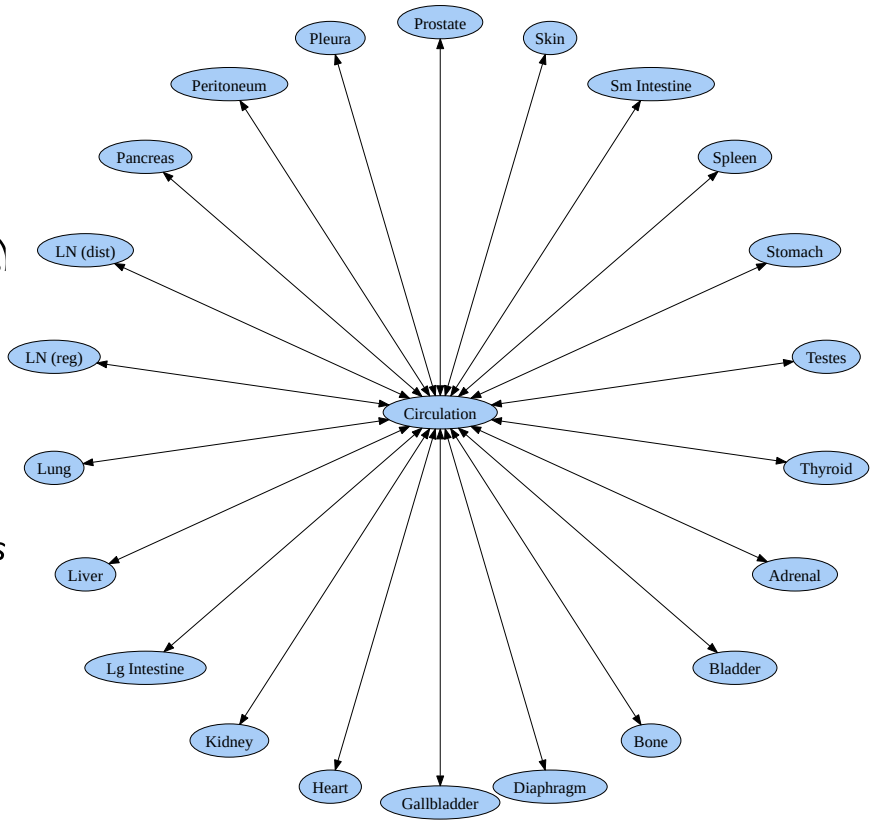

- 22 cell types
- Preoncogenic/Postoncogenic cancer Boolean (**True** or **False**)
- Each anatomical site has indigenous cell type
- Prostate is initially populated with cancerous & healthy cells

Cell Attributes

Location	1,…23 (including circulation)
Type	1,…22
Cell ID	1,…,n
Preonc/Postonc	Boolean: true/false

Birth time
Death time
Circulation time
Parent Cell
Previous Locations [1,23,2,23]

Primary Tumor Site: 1
[Primary tumor cancer cells]

Birth Rate	$\mu^{(1)}$
Death Rate	$\beta^{(1)}$
Mutation Rate	$\gamma^{(1)}$
Circulation Rate	$\lambda^{(1)}$

Secondary Sites: i = 2,…,22
[Healthy cells]

Birth Rate	$\mu^{(i)}$
Death Rate	$\beta^{(i)}$
Mutation Rate	$\gamma^{(i)}$
Circulation Rate	$\lambda^{(i)}$

23rd location is circulation

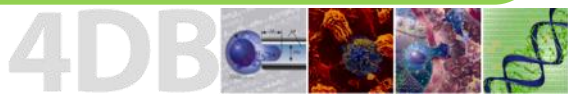

Entering Circulation

- Probability of entering entering site i

$$p_{(i)} = 1 - e^{-\lambda^{(i)} t}$$

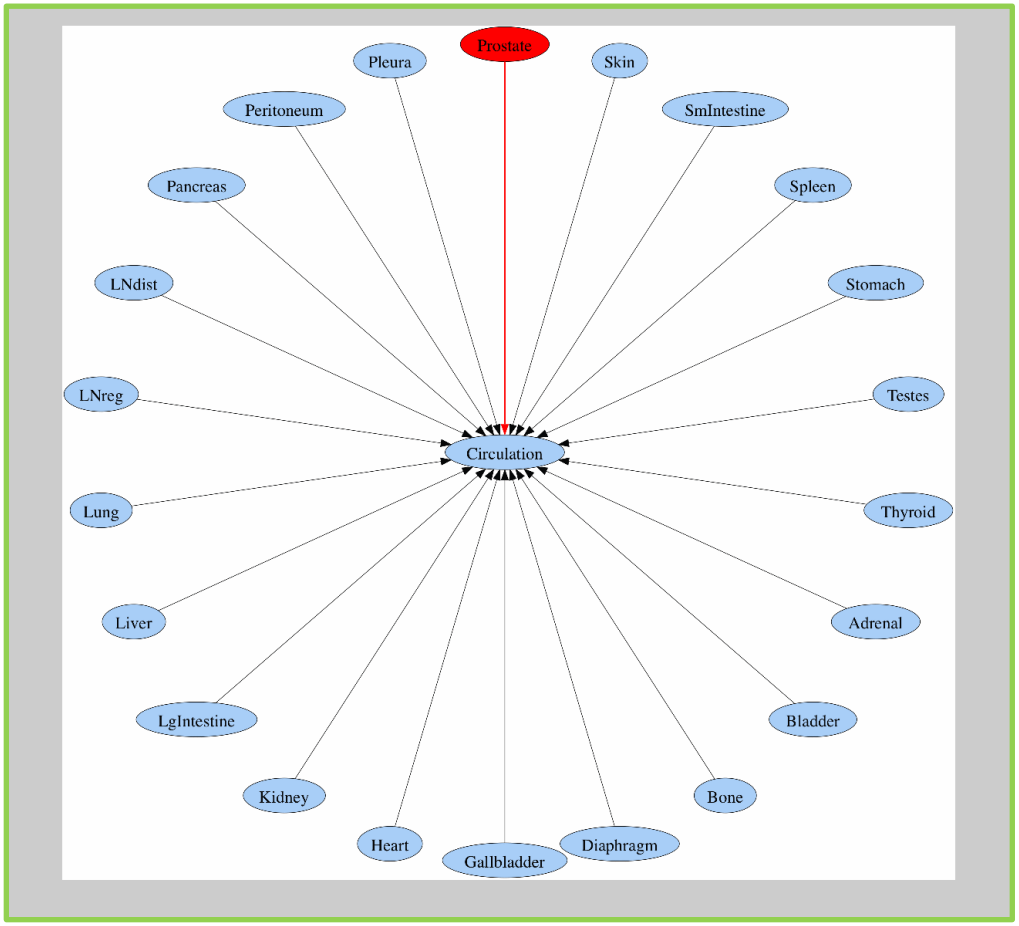

Dynamics in Circulation

- Holds many cell types at each time step
- Cell death can occur, but not birth
- No mutations
- No replicator equations

- Entering Circulation

$$p_{(i)} = 1 - e^{-\lambda^{(i)} t}$$

- Exiting Circulation
  - Based on Markov transition probabilities

- Preoncogenic Prostate Cell
- Postoncogenic Prostate Cell
- Healthy Prostate Cell
- Liver Cell

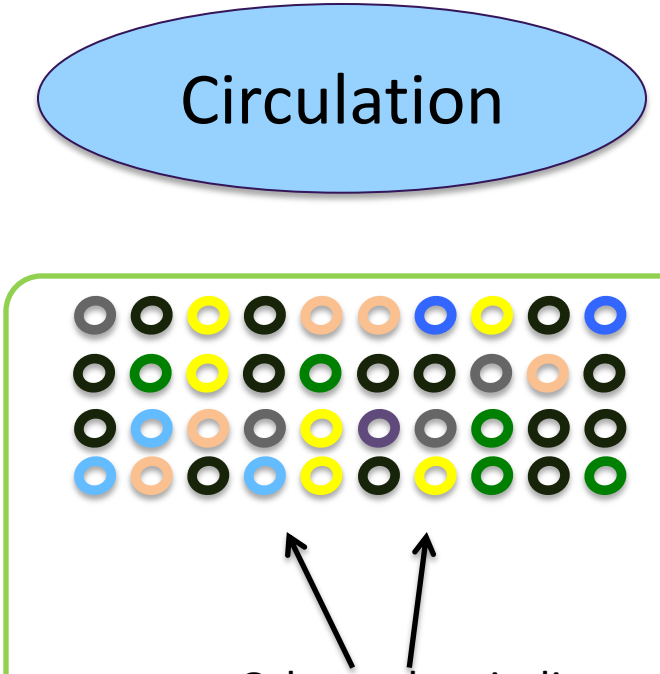

Circulation

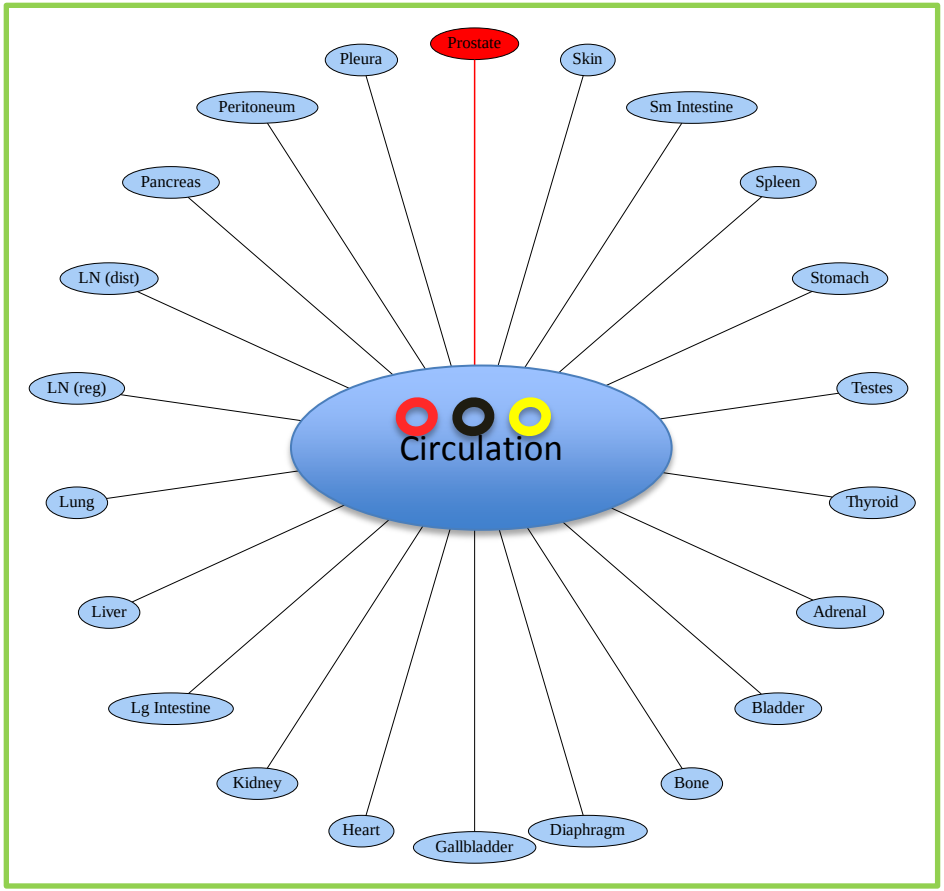

- Prostate

$$p_1 = 1 - e^{-\lambda^{(i)} t}$$

- Each anatomical site has indigenous cell type

Healthy Prostate Cell

Postoncogenic Prostate Cell

Liver Cell

Replicator Equations

- Large cell population of n types, proportions given by the state vector, whose components sum to 1:

$$\vec{x} = (x_1, x_2, ..., x_n) \in S_n$$

$$\sum_{i=1}^{n} x_i = 1$$

- Fitness landscape of cell type *i* given by:

$$f_i = (Ax)_i = a_{i1}x_1 + ... + a_{in}x_n$$

A = payoff matrix

Ex: $$A = \begin{bmatrix} 3 & 4 \\ 1 & 2 \end{bmatrix}$$

- Average fitness of the cell population:

$$\phi = \vec{x} \cdot \vec{f}$$

- Replicator equation describing cell population dynamics:

$$\dot{x}_i = \sum_{j=1}^{n} x_j f_j(\vec{x}) q_{ji} - \phi(\vec{x}) x_i$$

- Q is the mutation matrix
- Controls all mutation rates from type i to j.
- Each row must sum to 1.

Ex: Q allows no mutations. $$Q = \begin{bmatrix} 1 & 0 \\ 0 & 1 \end{bmatrix}$$

Neutral Payoff Matrix

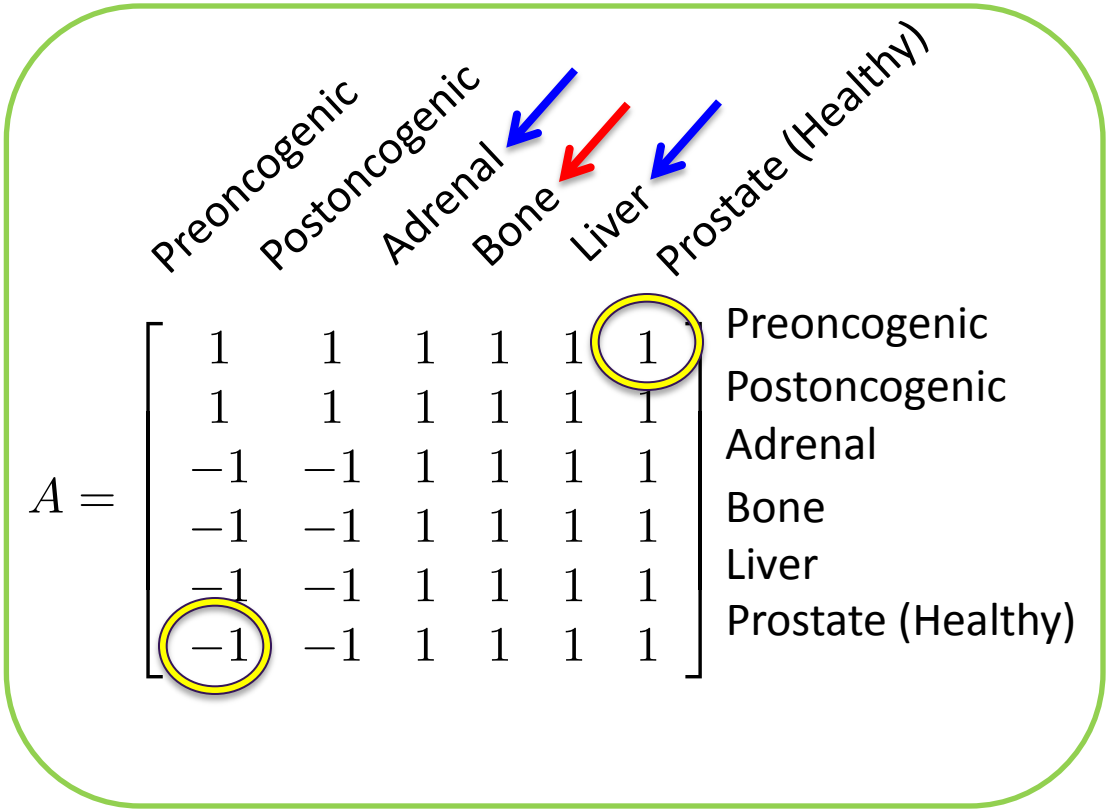

Sample Monte Carlo simulation

Circulation and mutation in sponges and spreaders

Adrenal

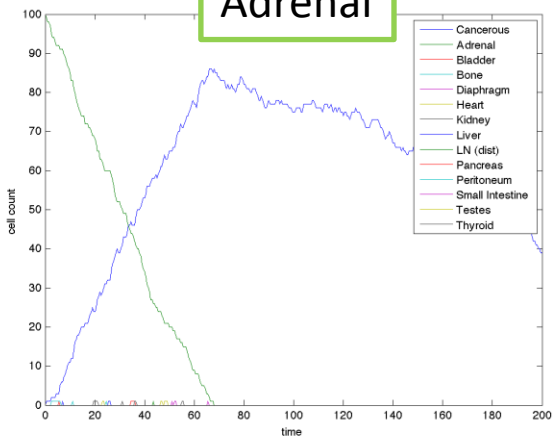

Bone

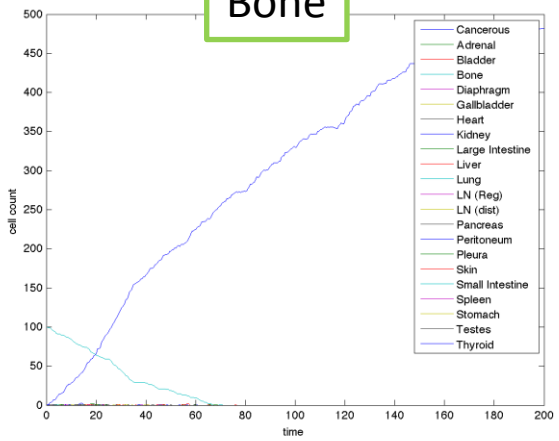

Circulation

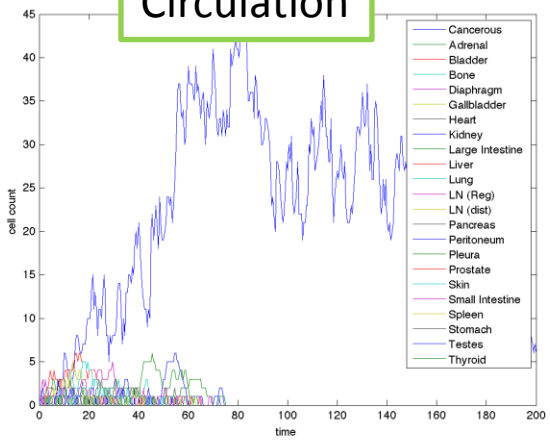

Parameter Values

- Mutation: 1.5
- Circulation: 1.0
- Remove from circulation: 1.5
- Birth/Death: 0
- Cancerous Birth: 0

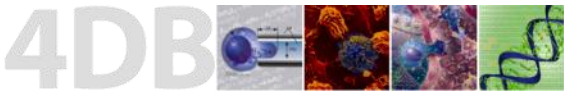

Questions?